

RIGA TECHNICAL UNIVERSITY

FACULTY OF MATERIAL SCIENCE AND APPLIED CHEMISTRY

**Māris KODOLS**

Doctoral student program “Materials science”

**THE DEVELOPMENT OF SYNTHESIS TECHNOLOGY OF ACTIVE  
TUNGSTATE PHOTOCATALYSTS**

**Summary of Doctoral Thesis**

Scientific Supervisor:

**Dr. habil. sc. ing. Jānis Grabis**

RIGA 2015

Kodols M. Development of the synthesis technology of active tungstate photocatalysts. Summary of the Doctoral Thesis. R.: RTU, 2015, 35 lpp.  
ISBN 978-9934-507-96-0

Printed in accordance with RTU Institute of Inorganic Chemistry resolution from 17.12.2014, protocol Nr. 2.



This work has been supported by the European Social Fund within the project “Support for the implementation of doctoral studies at Riga Technical University”.

**THE DOCTORAL THESIS IS SUBMITTED FOR AWARD OF DOCTORAL  
DEGREE IN ENGINEERING SCIENCES AT RIGA TECHNICAL  
UNIVERSITY**

The Thesis for the doctoral degree in engineering sciences is to be publicly defended on May 27<sup>th</sup> 2015, at the Riga Technical University, The Faculty of Material Science and Applied Chemistry, at conference hall (room Nr. 272).

**OFFICIAL REVIEWERS**

Dr. habil. phys., Baiba Bērziņa, Institute of Solid State Physics University of Latvia

Dr. phys., Jānis Kleperis, Institute of Solid State Physics University of Latvia

Dr. chem., Bruno Andersons, Latvian State Institute of Wood Chemistry

**CONFORMATION**

I confirm that I have developed the present Doctoral Thesis, which is submitted for consideration at Riga Technical University for scientific degree of the doctor of engineering sciences. The Doctoral Thesis has not been submitted at any other university for the acquisition of a scientific degree.

Māris Kodols ..... Date: .....

The doctoral Thesis is written in Latvian language, it contains Introduction, Review of the Literature, Methods, Discussion of Experiments, Conclusions, list of References, as well as 58 illustrations, 20 tables, 92 literature References are used for this Doctoral Thesis.

## ACKNOWLEDGEMENTS

I would like to thank my supervisor Dr. habil. sc. ing. Jānis Grabis for his support and motivation during the time while working on this Doctoral Thesis. I am thankful to all my colleagues of RTU Institute Of Inorganic Chemistry for supportive discussions, motivation, as well as practical hands and advices, especially Sabīne Didrihsone, Aija Krūmiņa, Astrīda Lipe Dzidra Jankoviča and Laura Rozenberga-Voska.

Special thanks to employees of “Rudolfs Cimdins Riga Biomaterial Innovation and Development Center of RTU” for opportunity to use scanning electron microscopy, especially Dagnija Loča, Dmitrijs Jakovļevs, Arita Dubņika and Inga Dušenkova. Special thanks to Zaiga Neidere, Guntars Kaspars and Vitālijs Freidenfelds for opportunity to make chromatographic analysis and for sharing their knowledge of chromatography data interpretation.

The inspiration, support and faith from my family have been immeasurable.

## CONTENTS

Overview of the Doctoral Thesis.....	6
State of the art and novelty.....	6
The aim of the Doctoral Thesis.....	6
Tasks to realize the aim of the Doctoral Thesis .....	6
Practical significance of the Doctoral Thesis .....	6
Novelty of the Doctoral Thesis .....	6
Approbation of the Doctoral Thesis .....	6
Review of the literature .....	7
Experimental methods .....	9
Determination of photocatalytic activity.....	10
Synthesis methods.....	11
Discussion of the results .....	13
1. Molten salt method.....	13
2. Sol-gel combustion synthesis .....	15
3. Hydrothermal and microwave synthesis .....	16
4. The influence of synthesis parameters on the crystallite sizes and specific surface area ....	17
5. The effect of sample thermal treatment on phase composition, specific surface area and crystallite sizes .....	20
6. The analysis of particle morphology .....	23
7. The summary of the synthesis methods .....	25
8. Evaluation of the photocatalytic activity of tungstates .....	26
9. The impact of particle morphology on the degradation of methylene blue .....	27
10. The influence of the specific surface area and crystallite size on the degradation of MB ...	28
11. The influence of the pH on the degradation of MB .....	29
12. Photocatalysis of reprocessed and regenerated samples .....	30
13. Evaluation of the MB degradation products.....	31
Conclusions .....	33
Thesis for defending .....	33
List of publications .....	34
List of conferences.....	34

## OVERVIEW OF THE DOCTORAL THESIS

### State of the art and novelty

The interest of nanosized tungstate particles and thin layers of ZnO-WO<sub>3</sub> and Bi<sub>2</sub>O<sub>3</sub>-WO<sub>3</sub> systems for use in photocatalysis, environment and energetic problems, as well as the luminescent materials and development of detectors have been studied for the last decades.

Zinc tungstate mostly is used for UV light region but the forbidden energy gap of bismuth tungstate allows using it at visible light ( $\lambda > 400$  nm), which makes an economically justified and advantageous group of photocatalysts. Both zinc tungstate and bismuth tungstate are intensively studied also as the semiconductors and ion conductors, which extends their usage.

However, the catalytic and luminescent properties are affected by degree of crystallization, structural defects, crystallite size, chemical and phase composition, modifiers and synthesis method. For the tungstate synthesis the mostly used methods are solid-state synthesis and different liquid phase reactions (sol-gel, hydrothermal, microwave, precipitation from salt solutions). The known methods are with low outcome and the results are controversial. The increase of the photocatalytic activity by developing optimal synthesis method and determining the phase content and chemical composition of the product, as well as crystallite size and role of modifiers, is an actual task.

**The aim of the Doctoral Thesis:** to develop the synthesis methods of active photocatalysts in oxide systems of ZnO-WO<sub>3</sub> and Bi<sub>2</sub>O<sub>3</sub>-WO<sub>3</sub> and to give recommendations about optimal composition, synthesis method and usage.

### Tasks to realize the aim of the Doctoral Thesis:

1. The synthesis of ZnWO<sub>4</sub> un Bi<sub>2</sub>WO<sub>6</sub> with different morphology
  - 1.1. Sol-gel combustion synthesis using different organic fuels, starting materials, thermal treatment;
  - 1.2. Microwave and hydrothermal synthesis;
  - 1.3. Synthesis in molten salts.
2. The photocatalytic activity of ZnWO<sub>4</sub> un Bi<sub>2</sub>WO<sub>6</sub> depending on obtaining method, specific surface area, crystallite size, morphology, pH;
3. ZnWO<sub>4</sub> and Bi<sub>2</sub>WO<sub>6</sub> modification metals, rare earth metals, oxides and their photocatalytic activity;
4. The optimization of suitable synthesis technique.

### Practical significance of the Doctoral Thesis

New information about the factors that determine the activity of tungstate photocatalysts has been obtained. As a result, the new synthesis technology with high outcome has been developed. Tungstate products have been obtained and detailed information of the photocatalysts for organic compound degradation has been studied. The study is important in design of materials in the field of environment protection.

### Novelty of the Doctoral Thesis

For the first time a single photocatalyst analysing method has been used in determination of various synthesis process, particle morphology parameters and the role of the development of effective photocatalysts. Acquired new knowledge about the formation of the tungstate in molten salts.

### Approbation of the Doctoral Thesis

The scientific achievements and main results of the scientific research of this Thesis have been presented in 18 international conferences, summarized in 9 full text scientific manuscripts.

## REVIEW OF THE LITERATURE

The rapid development of the technologies and human economical expansion is associated with alternative sources of energy as well as development of technologies with decrease of pollution. The use of the Sun energy and its transformation to more effective form has been known for years. The Sun collectors and Sun accumulators are one of the first energy transformation systems in 20<sup>th</sup> century and its development is still in progress. The role of the photocatalysts in degradation of the organic pollution has been studied more intensively.

The European Commission and European Union have set the sustainable environment and the decrease of the pollution as one of the priorities. Several programmes (SETIS, FW 7, COST Action 540) and guidelines that prescribe the direction of environment protection have been developed. The development of environmental technologies are one of the tasks which includes also studies of photocatalysis and adjusting for wastewater and air purification, as well as developing hydrogen energy. Several fields and strategies are highlighted for photocatalyst usage:

1. New material development for photochemistry and photocatalysis,
2. Development and formation of general principles of the photocatalysis,
3. Development of visible-light-driven photocatalysts,
4. The purification of water, air and soil, including solar technologies,
5. Self-cleaning surfaces,
6. Photo sensible antimicrobial materials,
7. The development of catalytic red-ox technologies,
8. Green synthesis using solar technologies,
9. The charge transfer dynamics and reaction mechanisms,
10. The commercial usage of photocatalysts.

Photocatalysis is one of the scientific directions, which has been already implemented in energetics, electronics, environmental engineering and chemical synthesis. During the 20<sup>th</sup> century the main principles of the photocatalysis have been defined by which in the presence of the light, the photocatalyst can split water molecule. Titania was the first described photocatalyst, which shows dual usage – water splitting by which can be obtained hydrogen and oxygen in gas form. Firstly this conceptually resolves one of the basic energetic problems not using the fossil energy sources. The second – Titania reduces organic and bacterial contamination by degrading pollution to CO<sub>2</sub> and H<sub>2</sub>O and improving the water quality and preserving the sustainable environment.

Potentially higher photocatalytic characteristics are for semiconductor oxide systems and most of the oxide systems have ability to respond to the ultraviolet and visible light irradiation. It is necessary to develop such oxide systems which photo response potential can be effectively exploited. Titania is active only in UV irradiation, which reduces its effectiveness. Since solar irradiation covers Earth with visible and infrared irradiation approximately 90% and with 10% of UV at upper atmospheric part, the important role in material sciences is the development of the material and synthesis technology, which could maximally use the solar energy. Several tungstates show photocatalytic ability in range of visible light. The photocatalysts in the oxide systems ZnO-WO<sub>3</sub> and Bi<sub>2</sub>O<sub>3</sub>-WO<sub>3</sub> are with potentially higher activity at UV range, as well as in visible light. Zinc and bismuth oxide systems and their hetero systems have been studied as photocatalysts and together in other compounds that expand their usage.

Concluding the review of the literature it is understood that the usage of the oxide systems ZnO-WO<sub>3</sub> and Bi<sub>2</sub>O<sub>3</sub>-WO<sub>3</sub> are growing. The most active development and studies of tungstate are in two directions – firstly from the synthesis technology point of view and secondly by improving the photocatalytic performance.

The synthesis technologies described in literature allows obtaining pure tungstate. However, the relations to the photocatalytic performance are controversial. From the synthesis technology point of view tungstate are obtained mostly by hydrothermal and sol-gel combustion synthesis. Sol-gel combustion synthesis is popular method but is shows relatively high agglomeration with several phase composition. In case of tungstate it is possible to reduce other phases by thermal calcination at temperature up to 900°C, which estimates the method as relatively ineffective.

Synthesis in molten salts is mostly described for similar compounds (i.e.  $\text{CaWO}_4$ ,  $\text{NiWO}_4$ ) and not covering the formation of tungstate in systems of  $\text{ZnO-WO}_3$  and  $\text{Bi}_2\text{O}_3\text{-WO}_3$ . Microwave synthesis allows obtaining high crystalline products and with relatively homogenous particle distribution, as well as small particle sizes.

The improvements of the photocatalytic abilities are devoted for doping zinc and bismuth tungstate with different elements (i.e. Eu, Cu, Ag, Cd, Fe, Pt) as well with conjugating with other systems (i.e. AgBr,  $\text{Ag}_2\text{O}$ , CdS,  $\text{PtCl}_4$ ). Usually the dopants are introduced in range of 0.1% - 5%. The connections with dopants and modifiers of tungstate band gap have been determined in several studies by reducing the band gap for use in visible light range.

The most used method for determination of the photocatalytic abilities are degradation of methylene blue that is admitted as effective method and included also as ISO standard method for photocatalytic characterization.

There is poor information about photocatalytic activities in relation to the particle morphology. The morphology analysis allows determining the relation between photocatalysts effectiveness and synthesis technology.

The photocatalytic process is influenced also by pH and the behaviour of the tungstate photocatalysts in different pH are poorly described.

As a result of the literature review, it has been concluded that tungstates are perspective group of photocatalysts and it is necessary to improve the studies in direction of synthesis technologies, as well as improving the photocatalytic abilities. Because of that the actual task is further development and optimization of the perspective synthesis techniques, including modification and improvement of photocatalytic performance.

## EXPERIMENTAL METHODS

Based on the review of the literature, four synthesis methods of tungstate are selected – molten salt synthesis, sol-gel combustion synthesis, microwave synthesis and hydrothermal synthesis. The experimental path is shown in Figure 1.

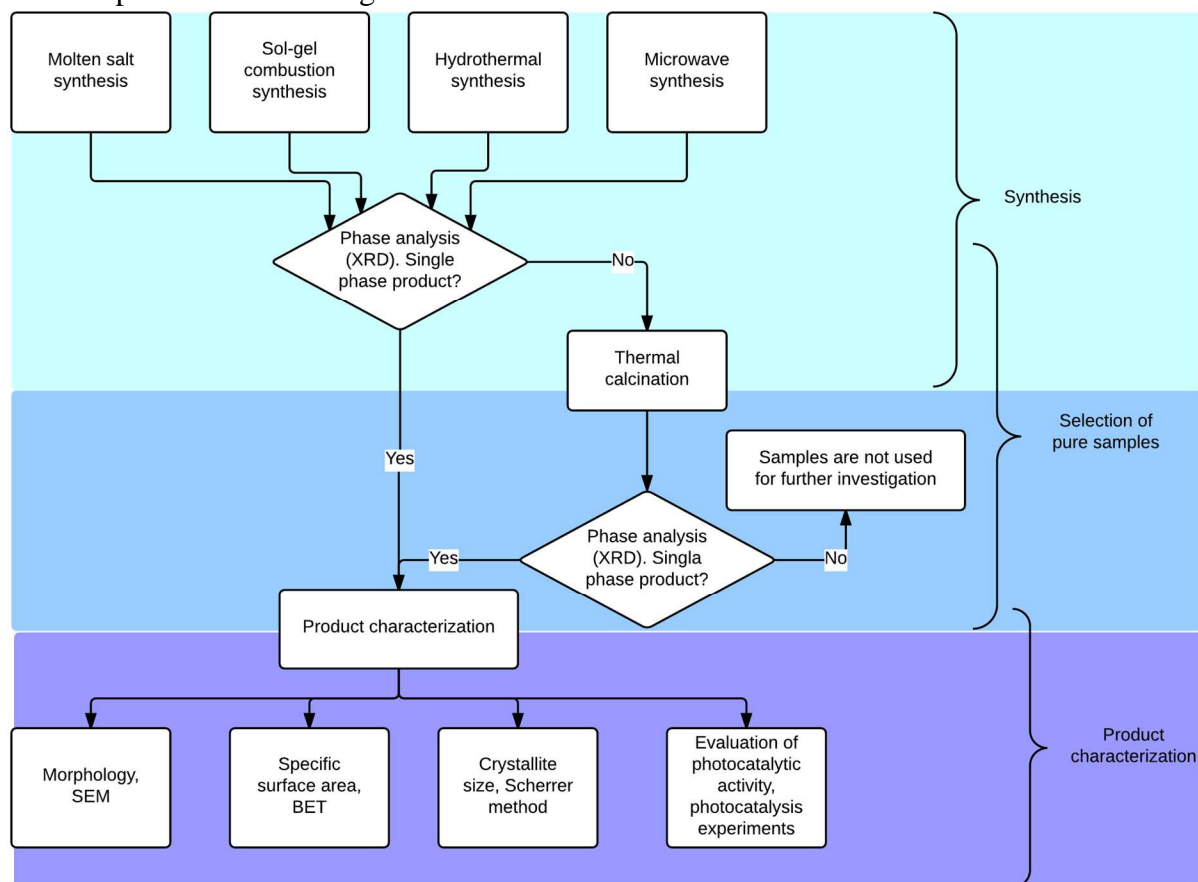


Fig.1. The experimental pathway

Since four different synthesis methods are selected for tungstate synthesis, for the better overviewing, the product batches are marked as following – batch A is obtained from molten salt synthesis, batch B are synthesized with sol-gel combustion method, batch C with hydrothermal synthesis, batch D is obtained with microwave synthesis. The systematic analysis are performed with different analysis methods and using sample calcination or by changing the synthesis parameters, new sample numbers applies.

Different synthesis methods give wider view of the tungstate synthesis and allow choosing optimal synthesis method for obtaining pure and effective products with controlled particle size. For synthesis environments the water and molten salts are used. By changing the synthesis environment and technique (Fig. 2), it is possible to influence the parameters of the photocatalysts.

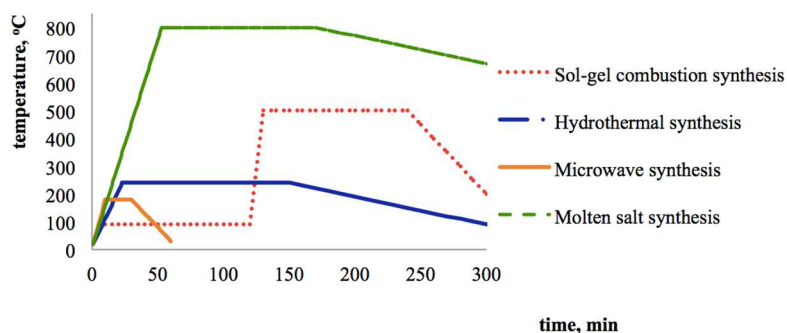


Fig. 2. The comparison of different synthesis techniques depending on synthesis temperature

Samples are analysed by using different methods – X-ray diffractometry (for determination of crystallite size and phase content), specific surface area using BET method, scanning electron microscopy (SEM) and transmission electron microscopy (TEM) for particle morphology analysis, differential thermal analysis for characterization of synthesis process, photocatalytic degradation of methylene blue dye and chromatographic methods for degradation product analysis.

#### Determination of photocatalytic activity

The photocatalytic activity of samples was assessed by degradation of methylene blue dye in the water with concentration of 0.0225 mmol/L. For typical analysis, the 0.2 g of photocatalyst is used. Quartz beaker with sample put under irradiation. For the first hour every 10 minutes ~3 mL of sample are taken and suspension is centrifuged and decanted. Absorption of solution is detected UV-VIS spectrophotometer at wavelength 664 nm corresponding to methylene blue spectra maxima. For the second hour samples are taken every 20 minutes.

Light sources:

- Mercury-quartz UV lamp FEK-56-PM, radiation range 185 – 365 nm, 120 W.
- Luminescence lamp Philips Tornado, 23 W (with spectral maxima of 435 nm and 548 nm), 1570 lm.
- Filter FC-1, 330 – 460 nm (with spectral maxima of 400 nm).

The degradation degree of methylene blue has been calculated using measured absorption at different time steps with following equations (1 and 2):

$$(1) c_t = \frac{A_t \cdot c_0}{A_0}$$

$$(2) S\% = \frac{c_t}{c_0} \cdot 100\%$$

$C_t$  – concentration of methylene blue, mmol/L, after time  $t$ , min;

$c_0$  – initial concentration of methylene blue, mmol/L;

$S\%$  - degree of the degradation of the methylene blue dye, %;

$A_t$  – sample absorption, Abs at different time steps  $t$ , min;

$A_0$  – initial absorption, Abs,  $t=0$ , min.

## Synthesis methods

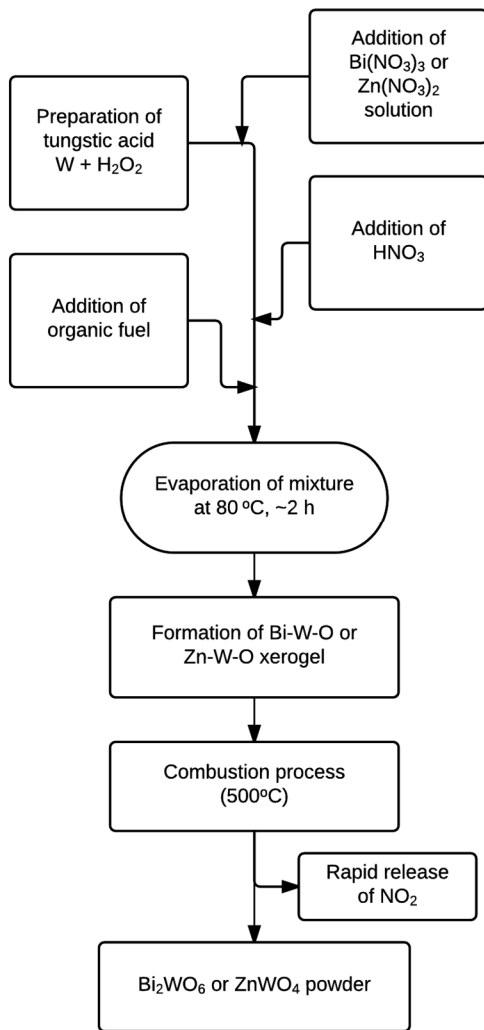


Fig.3. Synthesis scheme of tungstate using sol-gel combustion method

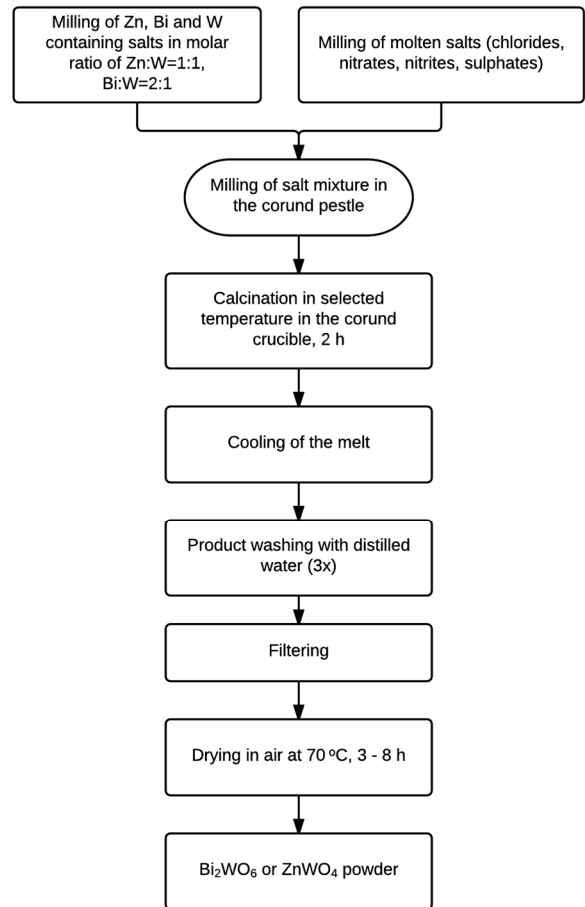


Fig.4. Synthesis scheme of tungstate using molten salt technique

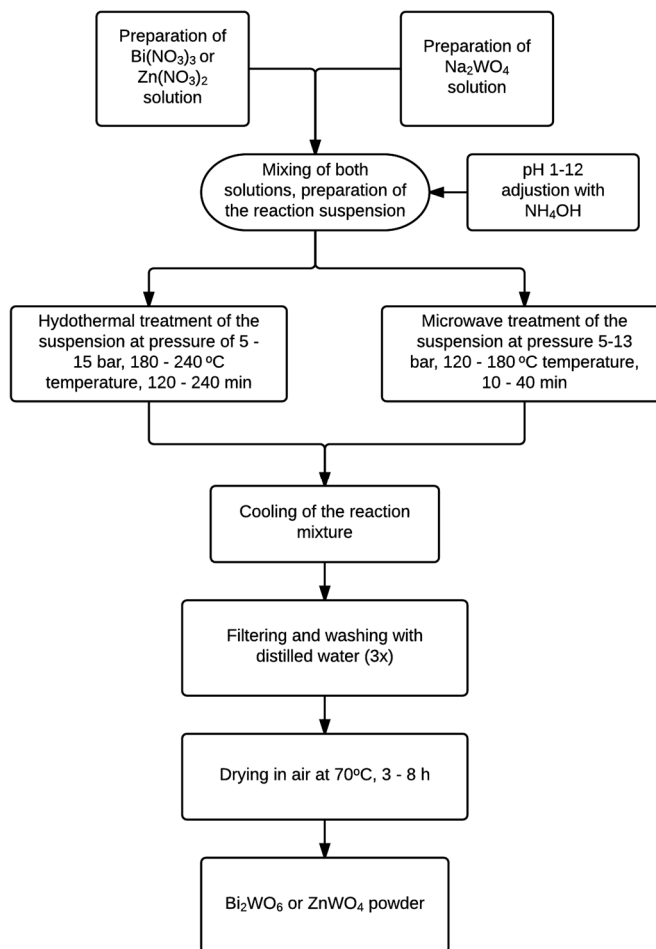


Fig. 5. Synthesis scheme of tungstate using microwave/hydrothermal method

The selected synthesis methods of the Bi<sub>2</sub>WO<sub>6</sub> and ZnWO<sub>4</sub> nanoparticles in comparison with such parameters as obtained product phase composition; specific surface area and crystallite size allows to conclude that optimal process parameters provides qualitative nanoparticles with similar parameters.

## DISCUSSION OF EXPERIMENTS

### 1. Molten salt method

The result of molten salt synthesis depends on used salts, which however is influenced by the temperature of the melt. The synthesis temperature was between 200 – 850°C. The product properties depending on molten salt synthesis regimes have been shown in Table 1.

Table 1

The phase content and properties of the product depending on molten environment and temperature

Oxide system	Sample	Molten salt environment	Synthesis temp., °C	Ratio prod./molt. salts	Specific surface area, m <sup>2</sup> /g	Crystallite size, nm	Phase composition
ZnO-WO <sub>3</sub>	A-1	LiNO <sub>3</sub>	268	1:1	-	-	ZnWO <sub>4</sub> , Li <sub>2</sub> WO <sub>4</sub> , Li <sub>6</sub> W <sub>2</sub> O <sub>9</sub> , ZnO
	A-2			1:2	-	-	ZnWO <sub>4</sub> , Li <sub>2</sub> WO <sub>4</sub> , Li <sub>6</sub> W <sub>2</sub> O <sub>9</sub> , ZnO
	A-3			1:4	-	-	Li <sub>2</sub> WO <sub>4</sub> , Li <sub>6</sub> W <sub>2</sub> O <sub>9</sub>
	A-4	NaNO <sub>3</sub>	350	1:1	28.5	28	ZnWO <sub>4</sub>
	A-5			1:2	28.0	25	
	A-6			1:4	26.9	27	
	A-7	KNO <sub>2</sub>	350	1:1	-	-	ZnO, WO <sub>3</sub> , W <sub>18</sub> O <sub>49</sub>
	A-8			1:2	-	-	ZnO
	A-9			1:4	-	-	ZnO
	A-10	NaCl-KCl	680	1:1	11.9	97	ZnWO <sub>4</sub>
	A-11			1:2	11.5	80	
	A-12			1:4	13.2	78	
	A-13	KCl	780	1:1	12.1	86	ZnWO <sub>4</sub> , ZnO (z)
	A-14			1:2	11.6	83	
	A-15			1:4	10.9	82	
	A-16	K <sub>2</sub> SO <sub>4</sub> - Na <sub>2</sub> SO <sub>4</sub>	850	1:1	9.5	74	ZnWO <sub>4</sub>
	A-17			1:2	10.9	100	
	A-18			1:4	8.7	110	
Bi <sub>2</sub> O <sub>3</sub> -WO <sub>3</sub>	A-19	LiNO <sub>3</sub> - NaNO <sub>3</sub>	200	1:1	-	-	WO <sub>3</sub>
	A-20			1:2	-	-	
	A-21			1:4	-	-	
	A-21	NaCl - NaNO <sub>3</sub>	310	1:1	-	-	BiOCl, WO <sub>3</sub>
	A-22			1:2	-	-	
	A-23			1:4	-	-	
	A-24	KNO <sub>2</sub>	350	1:1	28.1	35	Bi <sub>2</sub> WO <sub>6</sub> , Bi <sub>14</sub> W <sub>2</sub> O <sub>27</sub> (z)
				1:2	26.0	42	
				1:4	31.5	21	
				1:8	34.8	21	
	A-25	Na <sub>2</sub> CO <sub>3</sub> - Na <sub>2</sub> SO <sub>4</sub>	500	1:3	14.2	73	Bi <sub>2</sub> WO <sub>6</sub> , Bi <sub>14</sub> W <sub>2</sub> O <sub>27</sub> , Bi <sub>14</sub> WO <sub>24</sub> , WO <sub>3</sub>
	A-26	KCl	500	1:1	16.2	57	Bi <sub>2</sub> WO <sub>6</sub> , Bi <sub>14</sub> W <sub>2</sub> O <sub>27</sub>
	A-27	KCl - K <sub>2</sub> SO <sub>4</sub>	640	1:1	-	-	Bi <sub>14</sub> W <sub>2</sub> O <sub>27</sub> , Bi <sub>2</sub> WO <sub>6</sub> , K <sub>2</sub> CO <sub>3</sub>
	A-28			1:2	-	-	
	A-29			1:4	-	-	
A-30	KCl - K <sub>2</sub> CO <sub>3</sub>	640	1:1	-	-	Bi <sub>14</sub> W <sub>2</sub> O <sub>27</sub>	
A-31			1:2	-	-	Bi <sub>14</sub> W <sub>2</sub> O <sub>27</sub> ; Bi <sub>2</sub> O <sub>3</sub>	
A-32			1:4	-	-	Bi <sub>2</sub> O <sub>3</sub> ; BiO <sub>2</sub>	
A-33	BaCl <sub>2</sub> - KCl	670	1:1	-	-	BiOCl	

Oxide system	Sample	Molten salt environment	Synthesis temp., °C	Ratio prod./molt. salts	Specific surface area, m <sup>2</sup> /g	Crystallite size, nm	Phase composition
	A-34 A-35 A-36	K <sub>2</sub> CO <sub>3</sub> – NaNO <sub>3</sub>	710	1:1 1:2 1:4	- - -	- - -	Bi <sub>2</sub> O <sub>3</sub>
	A-37	NaCl – KCl	750	1:1	14.8	79	Bi <sub>2</sub> WO <sub>6</sub>
	A-38	KCl	800	1:1	12.2	33	Bi <sub>2</sub> WO <sub>6</sub>
	A-39	K <sub>2</sub> SO <sub>4</sub> – Na <sub>2</sub> SO <sub>4</sub>	831	1:1	13.9	87	Bi <sub>2</sub> WO <sub>6</sub>

The product composition obtained from molten salts, as well as specific surface area and crystallite size depends on the temperature, molten salt nature and their concentration. The influence of synthesis parameters of the ZnWO<sub>4</sub> or Bi<sub>2</sub>WO<sub>6</sub> obtaining is different.

Pure ZnWO<sub>4</sub> nanoparticles has been obtained using NaNO<sub>3</sub>, NaCl-KCl or K<sub>2</sub>SO<sub>4</sub>-Na<sub>2</sub>SO<sub>4</sub> as molten salt environment at temperatures 350°C, 680°C or 850°C, respectively. The specific surface area and crystallite size for zinc tungstate depends on the used synthesis temperature regime and less depending from the ratio between product and molten salts. The higher melting temperature promotes crystallite growing during synthesis and higher amounts of molten salt environment restrict the crystallite growing. The LiNO<sub>3</sub> and KNO<sub>2</sub> salts are not suitable for the synthesis of ZnWO<sub>4</sub>, because their low melting temperature is not tended for obtaining the desirable product. Pure ZnWO<sub>4</sub> with low amounts of ZnO as impurity can be obtained in KCl melt at 780°C, but higher temperature promotes crystallite growing and increases the cost of the process. The data in Table 1 shows that useful ZnWO<sub>4</sub> synthesis has been procured in NaNO<sub>3</sub> environment at 350°C temperature.

The evaluation of the molten salt synthesis for the bismuth tungstate obtaining shows that increase of the synthesis temperature promotes single-phase product. However, the nature of the molten salts also can influence the formation of different phase composition. For example, practically pure bismuth tungstate (sample A-24) with small amounts of Bi<sub>14</sub>W<sub>2</sub>O<sub>27</sub> as impurity (<1%) can be obtained in potassium nitrite at 350°C, but there are no tungstate identified below the 310°C of synthesis temperature (samples A-19 – A-23), because during the synthesis reaction, soluble compounds are formed which during filtering process has been washed away.

Pure bismuth tungstate (sample A-38) has been provided in the KCl melt; however, the primary evaluation was difficult because of crystal orientation and anisotropy. It can be seen that (hkl) reflexes 131, 151, 171, 191 shows decrease of intensities and increase of intensity of 002 reflex (the position of 2 $\theta$ ° is not changed). The specific crystal lattice of bismuth tungstate, which is orthorhombic, and with elongated c parameter can explain this. This tends to form plate type particles and causes the crystal orientations.

Bismuth tungstate is already formed during the grinding process, because of specific melting environment - potassium nitrite. The intensive reaction in the melting temperature (350°C) of potassium nitrite as oxidative reagent provides pure Bi<sub>2</sub>WO<sub>6</sub> (sample-A-24). Pure Bi<sub>2</sub>WO<sub>6</sub> has been obtained using NaCl-KCl at 750°C or KCl and K<sub>2</sub>SO<sub>4</sub>-Na<sub>2</sub>SO<sub>4</sub> molten salts at 800°C and 831°C temperatures, respectively. However, the specific surface area of the tungstate is not high and crystallite sizes are large.

It is predicted that phase composition, specific surface area and crystallite sizes are also changing by changing the ratio of the molten salt environment and product. The experimental results show slight dependence of the specific surface area and higher dependence of crystallite sizes by changing the ratio of product/ molten salts. This ratio slightly affects the phase composition, however, it is not relevant, because it is influenced only in multiphase samples, i.e., molten salt environments (samples A-1–A-3, A-7–A-9, A19–A-23, A-27–A-36) that are not effective for obtaining bismuth

and zinc tungstates. It is suggested to use NaCl-KCl, NaNO<sub>3</sub>, K<sub>2</sub>SO<sub>4</sub>-Na<sub>2</sub>SO<sub>4</sub> and NaCl-KCl or KCl, KNO<sub>2</sub> molten salts for obtaining single phase ZnWO<sub>4</sub> and Bi<sub>2</sub>WO<sub>6</sub>, respectively.

## 2. Sol-gel combustion synthesis

During sol-gel combustion synthesis experiments, the organic reagents and their ratio with nitrate ions (org/NO<sub>3</sub><sup>-</sup>) are changed, because of their role and impact on the impurities, specific surface area and crystallite sizes (Table 2).

Table 2

The characteristics of the samples obtained by sol-gel combustion synthesis

Oxide system	Sample	Synthesis parameters		Specific surface area, m <sup>2</sup> /g	Crystallite size, nm	Phase composition
		Organic fuel	Ratio org/NO <sub>3</sub> <sup>-</sup>			
Bi <sub>2</sub> O <sub>3</sub> -WO <sub>3</sub>	B-1	Citric acid	0.67	19.8	46	Bi <sub>2</sub> WO <sub>6</sub> Bi <sub>14</sub> W <sub>2</sub> O <sub>27</sub> ,
	B-2		0.50	17.8	58	Bi <sub>2</sub> WO <sub>6</sub> , Bi <sub>14</sub> W <sub>2</sub> O <sub>27</sub> , Bi <sub>14</sub> WO <sub>24</sub> (Z)
	B-3		0.33	12.5	64	Bi <sub>2</sub> WO <sub>6</sub> , Bi <sub>14</sub> W <sub>2</sub> O <sub>27</sub> , Bi <sub>14</sub> WO <sub>24</sub>
	B-4	Ethylene glycol	0.67	25.1	19	Bi <sub>2</sub> WO <sub>6</sub> , Bi <sub>14</sub> W <sub>2</sub> O <sub>27</sub> , Bi <sub>14</sub> WO <sub>24</sub> (Z)
	B-5		0.50	21.9	24	Bi <sub>2</sub> WO <sub>6</sub> , Bi <sub>14</sub> W <sub>2</sub> O <sub>27</sub> , Bi <sub>14</sub> WO <sub>2</sub>
	B-6		0.33	19.1	27	Bi <sub>2</sub> WO <sub>6</sub>
	B-7	Glycine	0.67	23.6	27	Bi <sub>2</sub> WO <sub>6</sub>
	B-8		0.50	15.1	31	Bi <sub>2</sub> WO <sub>6</sub> Bi <sub>14</sub> W <sub>2</sub> O <sub>27</sub>
	B-9		0.33	17.6	40	Bi <sub>2</sub> WO <sub>6</sub> Bi <sub>14</sub> W <sub>2</sub> O <sub>27</sub>
	B-10	Glycerine	0.67	24.8	28	Bi <sub>2</sub> WO <sub>6</sub>
	B-11		0.50	20.4	42	Bi <sub>2</sub> WO <sub>6</sub>
	B-12		0.33	19.6	32	Bi <sub>2</sub> WO <sub>6</sub>
ZnO-WO <sub>3</sub>	B-13	Citric acid	0.67	20.8	35	ZnWO <sub>4</sub>
	B-14		0.50	15.4	45	ZnWO <sub>4</sub>
	B-15		0.33	14.0	57	ZnWO <sub>4</sub>
	B-16	Ethylene glycol	0.67	18.2	40	ZnWO <sub>4</sub>
	B-17		0.50	17.1	42	ZnWO <sub>4</sub>
	B-18		0.33	14.1	51	ZnWO <sub>4</sub>
	B-19	Glycine	0.67	24.2	51	ZnWO <sub>4</sub>
	B-20		0.50	21.4	57	ZnWO <sub>4</sub>
	B-21		0.33	17.4	55	ZnWO <sub>4</sub>
	B-22	Ethanol	0.67	23.4	38	ZnWO <sub>4</sub>
	B-23		0.50	23.9	36	ZnWO <sub>4</sub>
	B-24		0.33	21.9	52	ZnWO <sub>4</sub>

The combustion synthesis using ethylene glycol, glycine or glycerine as organic fuels with ratio org/NO<sub>3</sub><sup>-</sup>=0.67 provides Bi<sub>2</sub>WO<sub>6</sub> with minimal crystallite size (19 – 28 nm) and high specific surface area (23.6 – 25.1 m<sup>2</sup>/g). While minimal crystallite sizes (35 – 40 nm) and maximum specific surface area (18.2 – 23.4 m<sup>2</sup>/g) for the ZnWO<sub>4</sub> are obtained using citric acid, ethanol or ethylene glycol as organic fuels at ratio org/NO<sub>3</sub><sup>-</sup>=0.67. Lower ratio of the org/NO<sub>3</sub><sup>-</sup> independently from used organic fuels increases the crystallite sizes and decrease specific surface area.

There are contradictory data in the literature about the impact of the organic fuels on the synthesis process. One of theories is based on the fast temperature change at ignition moment.

Higher amount of organic fuel tends fast temperature increase, which leads to faster synthesis process and ensures formation of the small crystallites. The release of higher amounts of the combustion by-products can limit the growing of the crystallites. There are lack of researches in case of tungstate synthesis, which support this interpretation, however the impact on the tungstate product composition using different organic fuels has been observed. It is determined that glycerine and glycine as organic fuels should be used for obtaining a single-phase bismuth tungstate in sol-gel combustion synthesis. In ZnO-WO<sub>3</sub> system pure zinc tungstate has been obtained by using of any studied organic fuels (samples B-16, B-13, B-19 and B-22). It should be noted that phase composition of the product depends not only on organic fuels but also on ratio org/NO<sub>3</sub><sup>-</sup>, which is responsible also for synthesis temperature. The evaluation of the ratio org/NO<sub>3</sub><sup>-</sup> change shows that increase to 0.67 increases also the specific surface area and it is concluded that higher ratio of org/NO<sub>3</sub><sup>-</sup> should be used in combustion synthesis.

The results show, that the sol-gel combustion synthesis method ensures formation of pure tungstate. The thermal treatment of products in higher temperatures decreases the amount of by-product impurities in samples, which can be explained by phase transition from non-stoichiometric tungstate to stoichiometric compounds. The harmful gas formation during the synthesis process can be noted as deficiency, however the advantage for this method is relatively low energy consumption and possibility to carry out synthesis in large amounts, which is relevant parameter on method's effectiveness.

### 3. Hydrothermal and microwave synthesis

The advantages of the hydrothermal and microwave synthesis are relatively low process temperature and increase of the pressure during synthesis. The x-ray analysis showed that both methods provide crystallise ZnWO<sub>4</sub> and Bi<sub>2</sub>WO<sub>6</sub> nanopowder formation. All diffractogramms shows widening of the diffraction reflexes, which confirms the small crystallite sizes. The characteristics of the products depending on hydrothermal and microwave synthesis parameters are shown on Table 3.

Table 3

The synthesis parameters of tungstate in hydrothermal and microwave synthesis

Oxide system	Sample	T, °C	Solution pH	Synthesis time, min	p, bar	Specific surface area, m <sup>2</sup> /g	Crystallite size, nm	Phase composition
ZnO-WO <sub>3</sub>	C-1	240	7	240	15	31,3	28	ZnWO <sub>4</sub>
	C-2	180	7	240	5	42,8	19	ZnWO <sub>4</sub>
	D-1	180	7	10	12	-	-	ZnO
	D-2	180	1	20	13	46,4	17	ZnWO <sub>4</sub>
	D-3	180	7	20	13	36,7	25	ZnWO <sub>4</sub>
	D-4	180	8	20	13	32,0	30	ZnWO <sub>4</sub>
	D-5	180	12	20	13	18,4	41	ZnWO <sub>4</sub>
	D-14	180	7	40	10	46,9	17	ZnWO <sub>4</sub>
	D-15	160	7	20	10	-	-	ZnO
D-16	120	7	20	10	-	-	ZnO	
Bi <sub>2</sub> O <sub>3</sub> -WO <sub>3</sub>	C-3	240	7	120	8	26,6	28	Bi <sub>2</sub> WO <sub>6</sub>
	C-4	180	7	240	8	22,6	35	Bi <sub>2</sub> WO <sub>6</sub>
	D-6	180	7	10	13	23,0	28	Bi <sub>2</sub> WO <sub>6</sub> , WO <sub>3</sub>
	D-7	180	1	20	13	29,8	17	Bi <sub>2</sub> WO <sub>6</sub>
	D-8	180	7	20	13	28,1	23	Bi <sub>2</sub> WO <sub>6</sub>
	D-9	180	8	20	13	26,5	32	Bi <sub>2</sub> WO <sub>6</sub>
	D-10	180	12	20	13	24,6	37	Bi <sub>2</sub> WO <sub>6</sub>
	D-11	180	7	40	10	24,0	35	Bi <sub>2</sub> WO <sub>6</sub>

Oxide system	Sample	T, °C	Solution pH	Synthesis time, min	p, bar	Specific surface area, m <sup>2</sup> /g	Crystallite size, nm	Phase composition
	D-12	160	7	20	13	-	-	Bi <sub>2</sub> WO <sub>6</sub> , WO <sub>3</sub>
	D-13	120	7	20	13	-	-	Bi <sub>2</sub> O <sub>3</sub>

Both synthesis methods provide ZnWO<sub>4</sub> and Bi<sub>2</sub>WO<sub>6</sub> at 180°C and higher temperatures, however the synthesis time is different. The necessary synthesis time for hydrothermal synthesis is 120 minutes but for microwave synthesis 20 minutes. The increase of crystallite size and decrease of specific surface area occurs in both synthesis methods by increasing duration and temperature during synthesis process. The parameters of the tungstate products are depending on pH and pressure during synthesis. The specific surface area of ZnWO<sub>4</sub> increases from 36.7 m<sup>2</sup>/g to 46.9 m<sup>2</sup>/g by changing pressure from 13 bar to 10 bar in microwave synthesis at 180°C temperature. Similar effect occurs by decreasing pressure from 15 bar to 5 bar in hydrothermal synthesis and by changing the temperature from 240°C to 180°C. This results in the higher specific surface area of ZnWO<sub>4</sub> from 31.3 m<sup>2</sup>/g to 42.8 m<sup>2</sup>/g and lowers crystallite sizes from 28 nm to 19 nm. The relevant impact by changing synthesis pressure of bismuth tungstate product parameters is not observed.

Comparing the sample parameters, which are obtained in the hydrothermal and microwave synthesis at 240°C and 180°C temperatures (samples C-1, D-3), respectively, at different synthesis times (240 and 20 minutes), it should be noted that ZnWO<sub>4</sub> with respective specific surface area 31.3 m<sup>2</sup>/g and 36.1 m<sup>2</sup>/g, have close crystallite sizes 28 and 25 nm, respectively. The Bi<sub>2</sub>WO<sub>6</sub> samples with highest specific surface area (29.8 m<sup>2</sup>/g) and smallest crystallite size (17 nm) has been obtained using microwave synthesis.

It is concluded that both synthesis methods provides pure tungstate formation at notably shorter time and more beneficial is microwave synthesis (synthesis time is shorten down to 20 min). The advantage for microwave synthesis is also the temperature regime, which does not exceed 180°C. The pH of environment is practically not relevant to product phase composition but influences the specific surface area and crystallite size. The higher specific surface area of product is obtained in acidic or neutral pH synthesis environment.

#### **4. The influence of synthesis parameters on the crystallite sizes and specific surface area**

It is determined that synthesis parameters of tungstate (temperature, synthesis time, pH, concentration ratio, organic fuel and nature of melt) influences not only phase composition but also crystallite sizes, particle morphology and specific surface area.

The crystallite sizes depending on synthesis method is shown in Figures 6 and 7. It can be seen that crystallite sizes for samples of batch A are increasing. Such tendency is because of synthesis temperature, which depends on used molten salts, consequently. It can be concluded that lower crystallite sizes can be obtained at lower temperature, for example 21 nm for bismuth tungstate sample A-24 and 28 nm for zinc tungstate sample A-4.

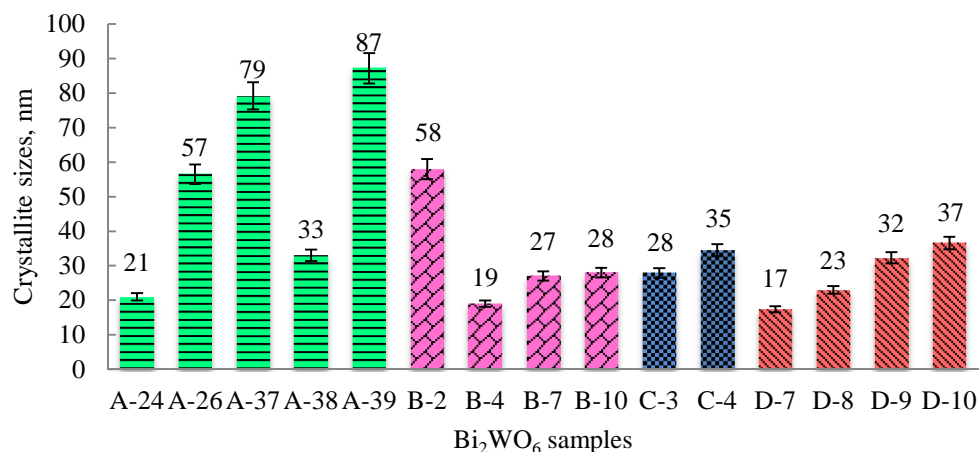


Fig. 6. Crystallite sizes of bismuth tungstate depending on synthesis method

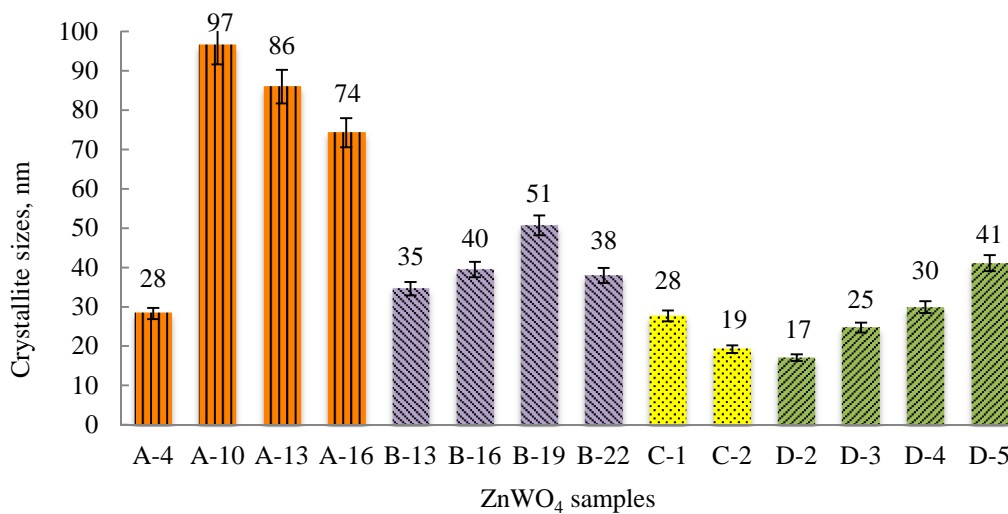


Fig. 7. Crystallite sizes of zinc tungstate depending on synthesis method

The highest crystallite sizes of 58 nm from batch B samples is obtained bismuth tungstate sample B-2. This sample has been synthesized using citric acid as organic fuel and the large crystallite sizes among the batch B can be explained with relatively stable metal complex formation during combustion synthesis, which is more difficult to combust and potentially has higher ignition temperature. It should be noted that x-ray analysis showed presence of impurity phase  $\text{Bi}_{14}\text{W}_2\text{O}_{27}$  in the sample B-2, which confirms that use citric acid is not effective for obtaining bismuth tungstate.

The sol-gel combustion synthesis (B samples) provides bismuth tungstate samples with crystallite sizes in range 19-58 nm (Fig. 6) but crystallite sizes for zinc tungstate samples are in range of 35-51 nm (batch B in Fig. 7). The sizes of crystallites during combustion synthesis are changing depending on composition of synthesis mixture – organic fuel and ratio with nitrate ions. It has been observed that crystallite sizes are decrease by the increase of the amount of organic fuels. For example, crystallite sizes are 27 nm for sample B-6 using org/ $\text{NO}_3^-$  ratio 0.33 but increasing this ratio up to 0.50 and 0.67, crystallites are tended to decrease up to 24 nm (sample B-5) and 19 nm (sample B-4). The explanation for such tendency is change of temperature during synthesis, because higher amount of organic fuels tends higher synthesis temperature and spontaneous small crystallite

formation following by that. Such observations can be seen on all B tungstate samples and can be concluded that for smaller crystallite sizes it suggested to use organic fuel ratio  $\text{org}/\text{NO}_3^-$  close to 0.67. It can be seen that samples obtained with ethylene glycol contains also by-products that can influence the growing of the crystallites.

The crystallite sizes of  $\text{Bi}_2\text{WO}_6$  samples are slightly larger than  $\text{ZnWO}_4$  samples which are hydrothermally synthesized. Microwave synthesis at  $180^\circ\text{C}$  temperature provides  $\text{Bi}_2\text{WO}_6$  and  $\text{ZnWO}_4$  with similar crystallite sizes of 17 nm, respectively. The process time of hydrothermal and microwave synthesis tends to small crystallite formation of tungstate comparing to molten salt and sol-gel combustion process.

The crystallite sizes correlates with specific surface area of samples obtained from combustion synthesis. As previously stated, the specific surface area has a tendency to decrease if the temperature is increasing. The reason for such tendency is because thermal treatment promotes recrystallization process and particle growing. Figures 8 and 9 shows the relation between different synthesis methods and change of specific surface areas.

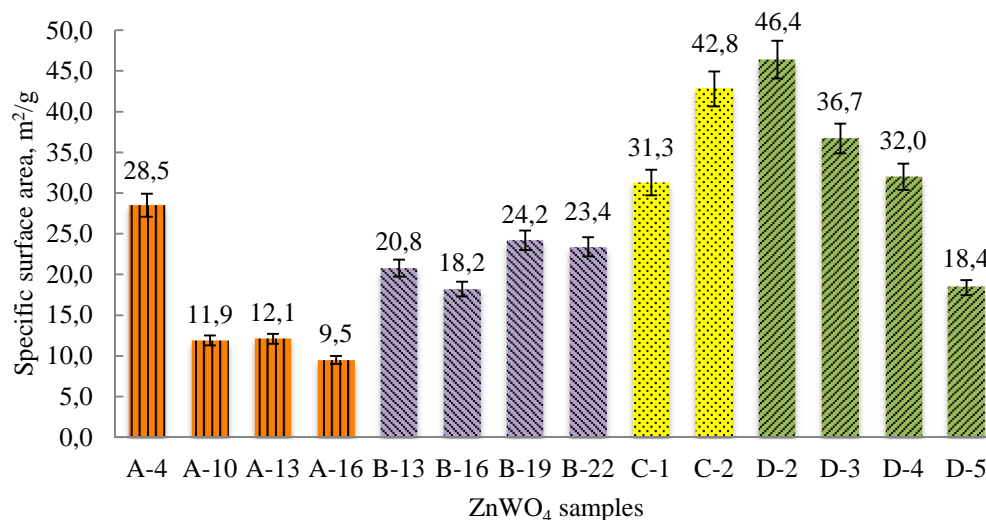


Fig. 8. Specific surface area of zinc tungstate depending on synthesis method

Figure 8 shows that zinc tungstate samples that are obtained at lower temperatures C ( $240^\circ\text{C}$ ), D ( $180^\circ\text{C}$ ) and A (sample A-4,  $350^\circ\text{C}$ ), has specific surface area above  $28.5 \text{ m}^2/\text{g}$  and reaches  $46.4 \text{ m}^2/\text{g}$ . It can be concluded that change of synthesis method zinc tungstate can be obtained with desired specific surface area up to  $46.4 \text{ m}^2/\text{g}$ . The most effective method in this case is microwave synthesis.

The bismuth tungstate samples have been obtained in wide range of specific surface area from  $12.2 \text{ m}^2/\text{g}$  (sample A-38) up to  $34.8 \text{ m}^2/\text{g}$  (sample A-24). Samples with higher specific surface area provides microwave synthesis ( $24.6 - 29.8 \text{ m}^2/\text{g}$ , C samples), hydrothermal synthesis ( $22.6 - 26.8 \text{ m}^2/\text{g}$ , D samples), sol-gel combustion synthesis ( $17.8 - 25.1 \text{ m}^2/\text{g}$ , B samples) and synthesis in molten  $\text{KNO}_2$  (sample A-24,  $34.8 \text{ m}^2/\text{g}$ ).

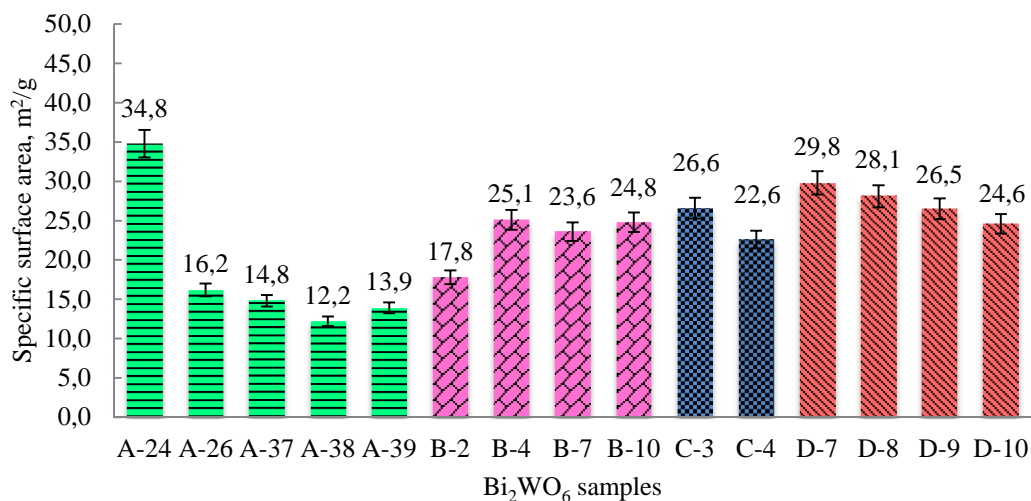


Fig. 9. Specific surface area of bismuth tungstate depending on synthesis method

The pH of synthesis environment influences the specific surface area and crystallite sizes of the samples. During microwave synthesis (D samples) the decrease of specific surface area is observed if pH increases (Fig. 10 and 11). At the same time, the pH does not affect the phase composition of the samples and in all cases pure tungstate has been obtained, but the maximum specific surface area is provided in acidic (pH 1 – 4) environment.

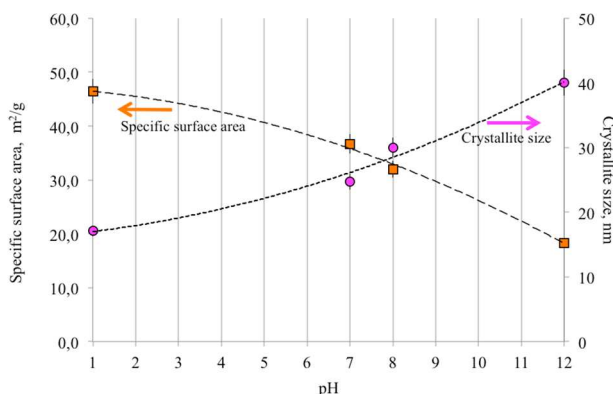


Fig. 10. The influence of pH on ZnWO<sub>4</sub> crystallite sizes and specific surface area in microwave synthesis

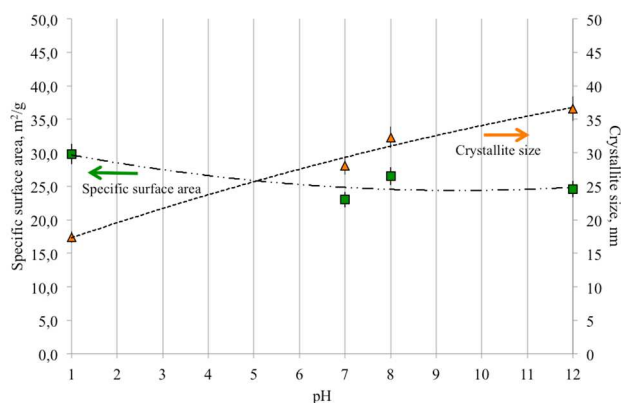


Fig. 11. The influence of pH on Bi<sub>2</sub>WO<sub>6</sub> crystallite sizes and specific surface area in microwave synthesis

It is concluded that optimal synthesis method for zinc tungstate and bismuth tungstate with high specific surface area and small crystallite sizes is microwave synthesis in acidic or neutral environment.

### 5. The effect of sample thermal treatment on phase composition, specific surface area and crystallite sizes

The thermal treatment was provided for all sol-gel combusted samples (Table 4) independently from initial phase composition. The thermal treatment promotes the increase of sample crystallinity. It has been seen that reaction during thermal treatment continuous and pure bismuth tungstate Bi<sub>2</sub>WO<sub>6</sub> forming from nonstoichiometric by-product phases Bi<sub>14</sub>W<sub>2</sub>O<sub>27</sub> and Bi<sub>14</sub>WO<sub>24</sub>. There are no

other phases observed during zinc tungstate synthesis, except on those cases when starting materials continuous reaction for complete ZnWO<sub>4</sub> formation.

Table 4

The phase composition, crystallite sizes and specific surface area depending on thermal treatment

Oxide system	Sample	Organic fuel	T, °C	Specific surface area, m <sup>2</sup> /g	Crystallite size, nm	Phase composition
Bi <sub>2</sub> O <sub>3</sub> -WO <sub>3</sub>	B-2	citric acid	500	17.8	58	Bi <sub>2</sub> WO <sub>6</sub> , Bi <sub>14</sub> W <sub>2</sub> O <sub>27</sub> , Bi <sub>14</sub> WO <sub>24</sub> (z)
			600	13.8	81	Bi <sub>2</sub> WO <sub>6</sub> , Bi <sub>14</sub> W <sub>2</sub> O <sub>27</sub> , Bi <sub>14</sub> WO <sub>24</sub> (z)
			700	9.8	147	Bi <sub>2</sub> WO <sub>6</sub> , Bi <sub>14</sub> W <sub>2</sub> O <sub>27</sub> (z)
			800	6.9	115	Bi <sub>2</sub> WO <sub>6</sub>
	B-4	Ethylene glycol	500	25.1	19	Bi <sub>2</sub> WO <sub>6</sub> , Bi <sub>14</sub> W <sub>2</sub> O <sub>27</sub> , Bi <sub>14</sub> WO <sub>24</sub> (z)
			600	16.7	73	Bi <sub>2</sub> WO <sub>6</sub> , Bi <sub>14</sub> W <sub>2</sub> O <sub>27</sub>
			700	12.9	116	Bi <sub>2</sub> WO <sub>6</sub> , Bi <sub>14</sub> W <sub>2</sub> O <sub>27</sub> (z)
			800	6.1	89	Bi <sub>2</sub> WO <sub>6</sub>
	B-7	Glycine	500	23.6	27	Bi <sub>2</sub> WO <sub>6</sub>
			600	18.6	40	Bi <sub>2</sub> WO <sub>6</sub>
			700	11.5	89	Bi <sub>2</sub> WO <sub>6</sub>
			800	5.8	95	Bi <sub>2</sub> WO <sub>6</sub>
	B-10	Glycerine	500	24.8	28	Bi <sub>2</sub> WO <sub>6</sub>
			600	20.4	44	Bi <sub>2</sub> WO <sub>6</sub>
			700	13.3	76	Bi <sub>2</sub> WO <sub>6</sub>
			800	6.1	89	Bi <sub>2</sub> WO <sub>6</sub>
ZnO-WO <sub>3</sub>	B-13	Citric acid	500	20.8	35	ZnWO <sub>4</sub>
			600	15.8	47	ZnWO <sub>4</sub>
			700	10.5	69	ZnWO <sub>4</sub>
			800	7.6	95	ZnWO <sub>4</sub>
	B-16	Ethylene glycol	500	32.0	40	ZnWO <sub>4</sub>
			600	27.0	42	ZnWO <sub>4</sub>
			700	25.0	57	ZnWO <sub>4</sub>
			800	22.0	68	ZnWO <sub>4</sub>
	B-19	Glycine	500	14.2	51	ZnWO <sub>4</sub>
			600	6.2	116	ZnWO <sub>4</sub>
			700	5.9	122	ZnWO <sub>4</sub>
			800	5.3	136	ZnWO <sub>4</sub>
	B-22	Ethanol	500	29.0	38	ZnWO <sub>4</sub>
			600	25.8	54	ZnWO <sub>4</sub>

Oxide system	Sample	Organic fuel	T, °C	Specific surface area, m <sup>2</sup> /g	Crystallite size, nm	Phase composition
			700	15.2	78	ZnWO <sub>4</sub>
			800	12.5	94	ZnWO <sub>4</sub>

z – signs, below quantifying limit

Taking into account that one of relevant parameters of photocatalysts are specific surface area and crystallite sizes, it is important to analyse these parameters, because of their important role in the formation of active sites onto the photocatalyst surface. Crystallite size increases at the higher temperatures, which is explained by the recrystallization process, when smaller crystallites fuse together. This effect can be seen in Figures 12 and 13.

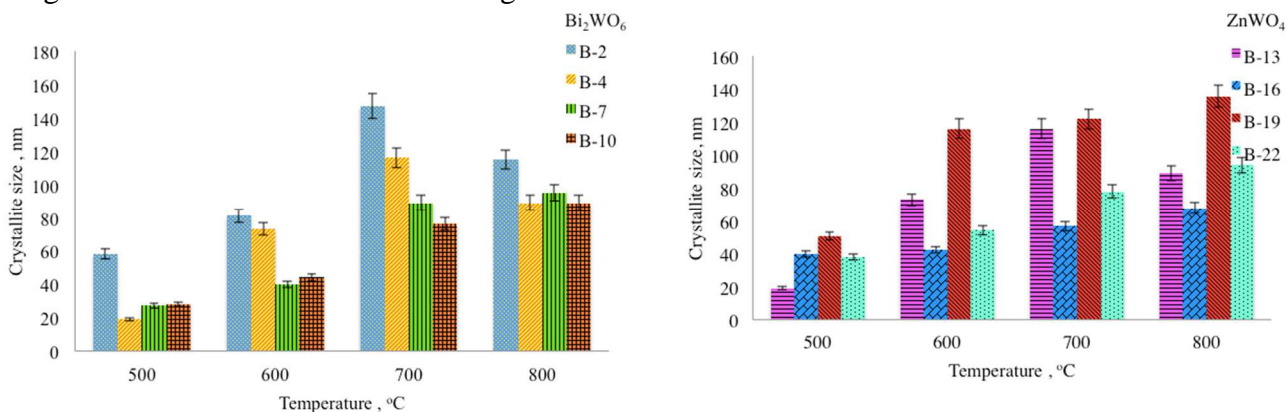


Fig. 12. Specific surface area and crystallite sizes of bismuth and zinc tungstate depending on temperature

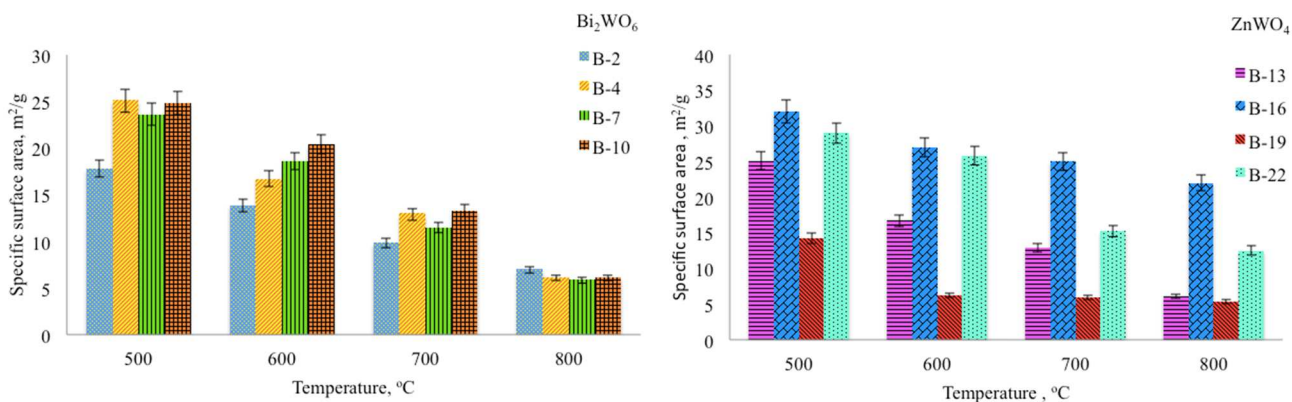


Fig. 13. Specific surface area and specific surface area of bismuth and zinc tungstate depending on temperature

In some cases there are observed tendency that crystallites are decreasing after increase during thermal calcination process (samples B-2, B-4, B-13). This effect is not widely studied. However, it can be assumed that firstly the recrystallization occurs and secondly there are several polymorphs of Bi<sub>2</sub>WO<sub>6</sub> at higher temperatures, which can lead to lattice changes and from this point of view it can result in such effect. Also there is possibility of amorphous phase formation during recrystallization process that can lead to the decrease of average crystallite sizes.

## 6. The analysis of particle morphology

In order to evaluate the effect of synthesis method and temperature the analysis of particle morphology has been made. It is predicted that by changing the tungstate synthesis method also the particle morphology changes. The overview of the agglomerated particles depending from synthesis obstacles and temperature has been described in further pictures.

Molten salt synthesis in 680 – 850°C temperatures provides agglomerated  $ZnWO_4$  samples (A-10, A-13 un A-16) with tamped and layered structures (Fig 14).

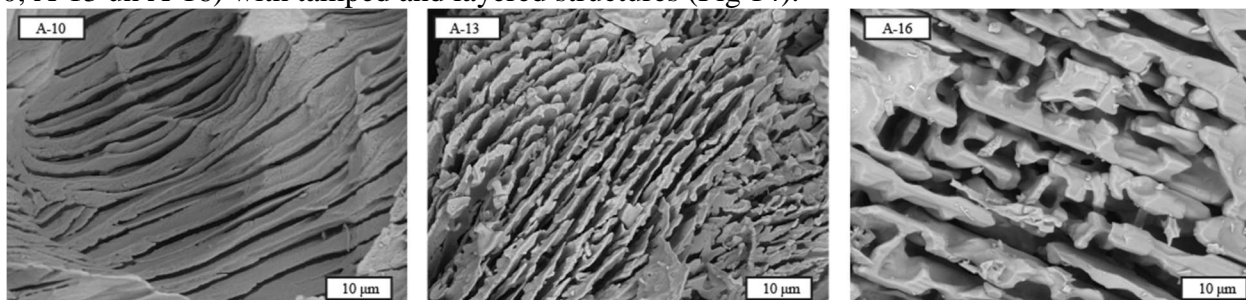


Fig. 14. Morphology of the layered structures of  $ZnWO_4$  samples A-10, A-13 and A-16

It is difficult to determine independent particle sizes and forms in these structures. It can be assumed that higher temperature promotes fused structure formation. There are irregular or needle shape particles obtained lower temperature (350°C) in  $NaNO_3$  as molten salt. This shows that lower synthesis temperature limit the formation of the aggregates.  $Bi_2WO_6$  samples that are obtained in molten salts have elongated plate like structures, which are formed from orthorhombic crystals with one elongated plane (Fig. 15). The effect of anisotropy was supported also by x-ray diffractograms.

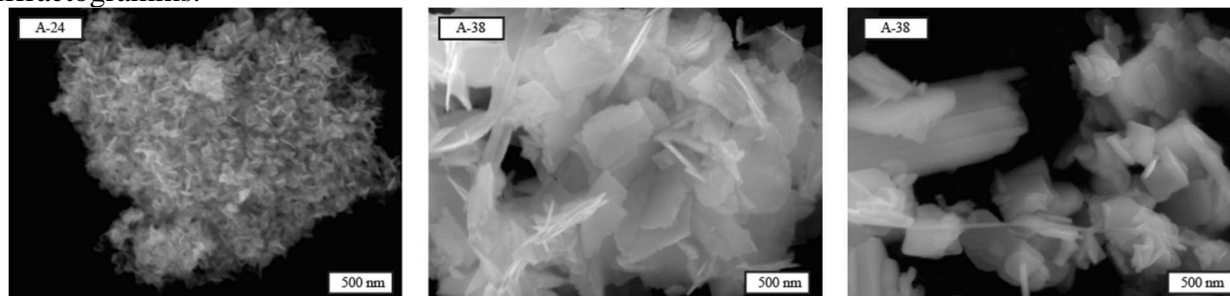


Fig.15. Morphology of the  $Bi_2WO_6$  samples A-24 and A-38 obtained from molten salts

Sol-gel combustion synthesis provides  $Bi_2WO_6$  samples with porous, sponge type agglomerates without restricted particle boundaries. The form of aggregates is slightly depending from used organic fuel, while further thermal treatment at 800°C enlarges the size of aggregates and independent particles have been observed. The  $ZnWO_4$  samples which are obtained with sol-gel combustion method, shows rounded and rod type particles, which are combined in porous agglomerates (Fig. 16).

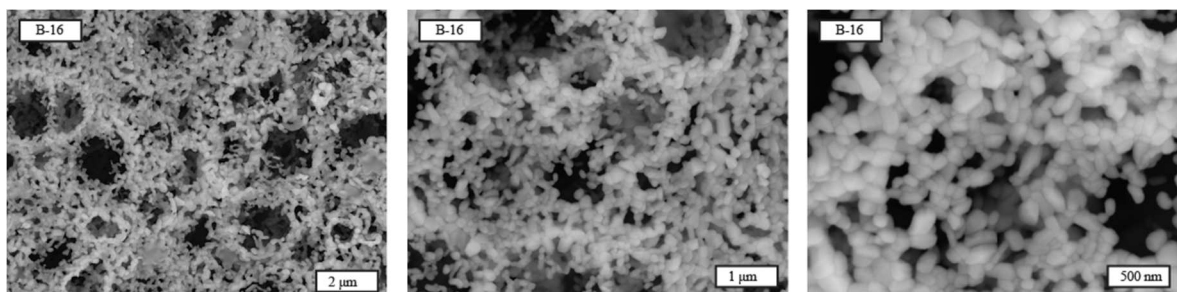


Fig. 16. Morphology of  $\text{ZnWO}_4$  sample B-16 at different magnifications

The hydrothermal synthesis at  $240^\circ\text{C}$  temperature provides relatively large particles ( $0,2 - 2 \mu\text{m}$ ) with flowerlike or flake like structure. Further calcination up to  $800^\circ\text{C}$  gradually enlarges particle or their aggregate size and changes the morphology (fig. 17).

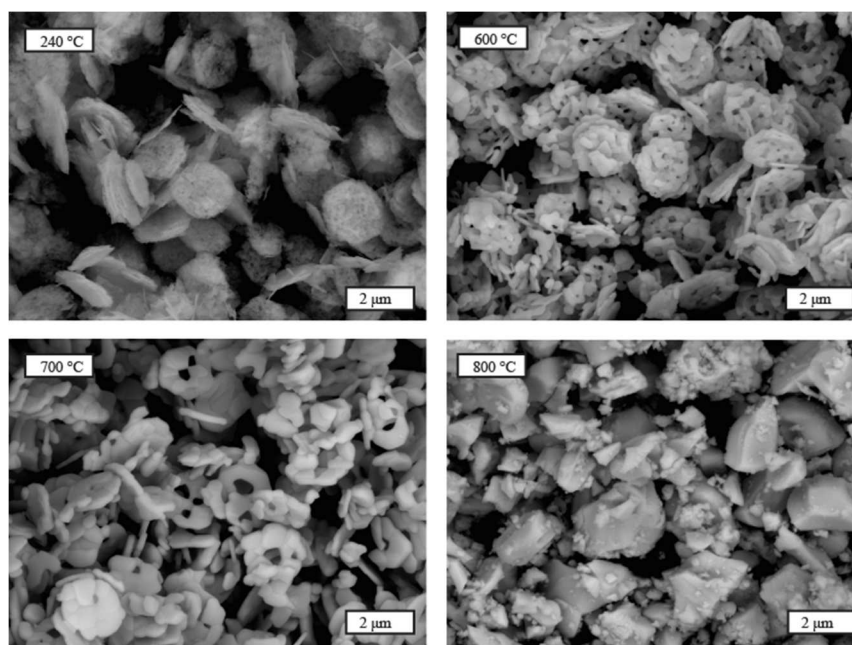


Fig. 17. Morphology of  $\text{Bi}_2\text{WO}_6$  sample C-3 that is obtained in hydrothermal synthesis and further calcination

The lower temperature of microwave synthesis and shorter synthesis time promotes spherical  $\text{ZnWO}_4$  nanoparticle formation ( $<30-40 \text{ nm}$ ) with uniform particle distribution, unlike, the  $\text{ZnWO}_4$  rod type particles (length up to  $150 \text{ nm}$ , diameter  $\sim 25-30 \text{ nm}$ ) that are obtained with hydrothermal synthesis method (Fig. 19).  $\text{Bi}_2\text{WO}_6$  aggregates consist of small flake like and needle type particles (Fig. 18).

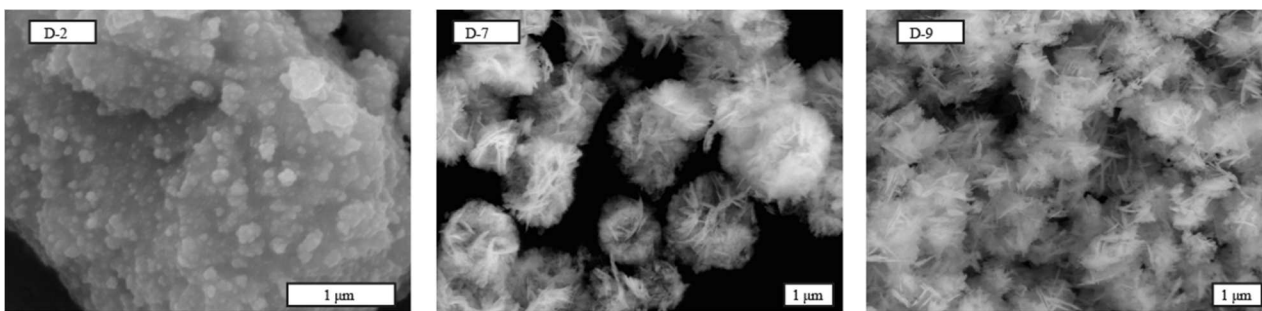


Fig. 18. Morphology of  $\text{ZnWO}_4$  sample D-2 and  $\text{Bi}_2\text{WO}_6$  samples D-7 and D-9 particle agglomerates, which are obtained in microwave synthesis

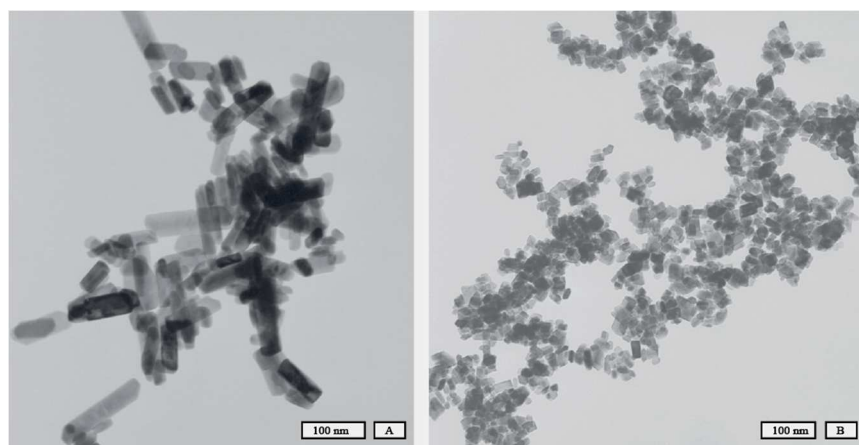


Fig. 19.  $\text{ZnWO}_4$  nanoparticles, which are obtained in hydrothermal (A) and microwave synthesis (B)

The studies with scanning electron microscopy shows that all tungstate nanoparticles has a tendency to agglomerate and form aggregates. By the formation of agglomerates it is difficult to determine real particle sizes. However, the apparent particle size of tungstate noticeably exceeds the crystallite sizes, because particles can consist of several crystallites.

## 7. The summary of the synthesis methods

The recommended synthesis parameters for obtain tungstate in molten salts.

1. The synthesis of  $\text{Bi}_2\text{WO}_6$  nanoparticles with specific surface area of  $31.5 - 34.8 \text{ m}^2/\text{g}$  and crystallite size about 21 nm should be provided in molten  $\text{KNO}_2$  at  $350^\circ\text{C}$ , at the ratio of product/melt from 1:4 to 1:8.
2. The synthesis of  $\text{ZnWO}_4$  nanoparticles with specific surface area of  $28.5 \text{ m}^2/\text{g}$  and crystallite size 25 – 28 nm should be provided in molten  $\text{NaNO}_3$  at  $350^\circ\text{C}$ , at the ratio of product/melt from 1:2 – 1:4.

The recommended synthesis parameters for obtain tungstate in sol-gel combustion synthesis.

1. The synthesis of  $\text{Bi}_2\text{WO}_6$  nanoparticles with specific surface area of  $23.6 - 24.8 \text{ m}^2/\text{g}$  and crystallite size 27 – 28 nm should be provided using glycine or glycerine as organic fuel, with ratio  $\text{org}/\text{NO}_3^-$  of 0,67.
2. The synthesis of  $\text{ZnWO}_4$  nanoparticles with specific surface area of  $20.8 - 23.9 \text{ m}^2/\text{g}$  and crystallite size 34 – 38 nm should be provided using citric acid or ethanol as organic fuel, with ratio  $\text{org}/\text{NO}_3^-$  of 0,67.

The recommended synthesis parameters for obtain tungstate using hydrothermal technique.

1. The synthesis of  $\text{Bi}_2\text{WO}_6$  nanoparticles with specific surface area of  $26.6 \text{ m}^2/\text{g}$  and crystallite size  $27 \text{ nm}$  should be provided at  $180 - 240^\circ\text{C}$ ,  $8 \text{ bar}$  pressure,  $\text{pH } 7$ , in  $240 \text{ min}$ .
2. The synthesis of  $\text{ZnWO}_4$  with specific surface area of  $42.8 \text{ m}^2/\text{g}$  and crystallite size  $20 \text{ nm}$  should be provided at  $180^\circ\text{C}$ ,  $5 \text{ bar}$  pressure,  $\text{pH } 7$ , in  $240 \text{ min}$ .

The recommended synthesis parameters for obtain tungstate using microwave synthesis.

1. The synthesis of  $\text{Bi}_2\text{WO}_6$  with specific surface area of  $29.8 \text{ m}^2/\text{g}$  and crystallite size  $17 \text{ nm}$  should be provided at  $180^\circ\text{C}$ ,  $13 \text{ bar}$  pressure,  $\text{pH } 1-7$ , in  $40 \text{ min}$ .
2. The synthesis of  $\text{ZnWO}_4$  with specific surface area of  $46.9 \text{ m}^2/\text{g}$  and crystallite size  $17 \text{ nm}$  should be provided at  $180^\circ\text{C}$ ,  $10 \text{ bar}$  pressure,  $\text{pH } 7$ , in  $40 \text{ min}$ .

Although all the used synthesis methods provides obtaining tungstate nanoparticles, the hydrothermal and microwave synthesis gives significant savings of working time and electricity, because of single step process, lower temperatures and shorter synthesis time. However, the dependence of particle morphology and possible defects in crystal structure using different synthesis techniques can tend the tungstate photocatalytic activity. Therefore the optimal synthesis technique can be provided after photocatalysis assessment.

## 8. Evaluation of the photocatalytic activity of tungstates

Usually the adsorption onto the catalysts surface decreases the methylene blue concentration approximately for  $20\%$  and the precondition before further analysis should be accomplished. Experimentally it is determined that samples should be processed and dispersed in the dark for approximately  $30 \text{ minutes}$  before absorption measurements because the adsorption of methylene blue on the catalysts surface is one of the first steps and the equilibrium concentration should be reached in the solution. The samples and their characteristics for photocatalytic experiments are listed in Table 5.

Table 5

The used samples in photocatalytic experiments

Oxide system	Sample	Specific surface area, $\text{m}^2/\text{g}$	Crystallite size, $\text{nm}$	Particle description
$\text{Bi}_2\text{O}_3\text{-WO}_3$	A-24 (1:2)	26.0	42	Layered agglomerates
	B-6	19.1	40	Porous agglomerates
	B-7	23.6	27	Porous agglomerates without strict grain boundaries
	B-10 ( $500^\circ\text{C}$ )	24.8	28	Porous agglomerates without strict grain boundaries
	B-11 ( $500^\circ\text{C}$ )	20.4	40	Agglomerates
	B-10 ( $700^\circ\text{C}$ )	13.3	74	Agglomerates
	B-10 ( $800^\circ\text{C}$ )	6.1	89	Agglomerates
	C-3	26.6	28	Flake/flower like particles
	D-9	26.5	32	Needle like particles
$\text{ZnO-WO}_3$	A-4	28.5	28	Needle like particles
	B-13 ( $500^\circ\text{C}$ )	20.8	35	Spherical agglomerates
	B-13 ( $600^\circ\text{C}$ )	15.8	47	Spherical agglomerates
	B-13 ( $700^\circ\text{C}$ )	10.5	69	Spherical agglomerates
	B-13 ( $800^\circ\text{C}$ )	7.6	95	Spherical agglomerates
	B-16	25.0	39	Spherical agglomerates
	B-25	27.4	24	Agglomerates
	C-1	31.3	28	Spherical particles
D-2	46.4	17	Fine spherical particles	

## 9. The impact of particle morphology on the degradation of methylene blue

There are significant changes for sample photocatalytic activities depending on particle morphology but with relatively similar specific surface area (for bismuth tungstate in SSA range of 24.8 – 26.6 m<sup>2</sup>/g, for zinc tungstate 27.4 – 46.4 m<sup>2</sup>/g respectively). From the literature review it has been studied that activity of catalysts can be affected by the distribution and binding of the oxygen atom on the surface of the catalyst, which means that surface topology can substantially change also photocatalytic activity, which is shown in Figure 6.

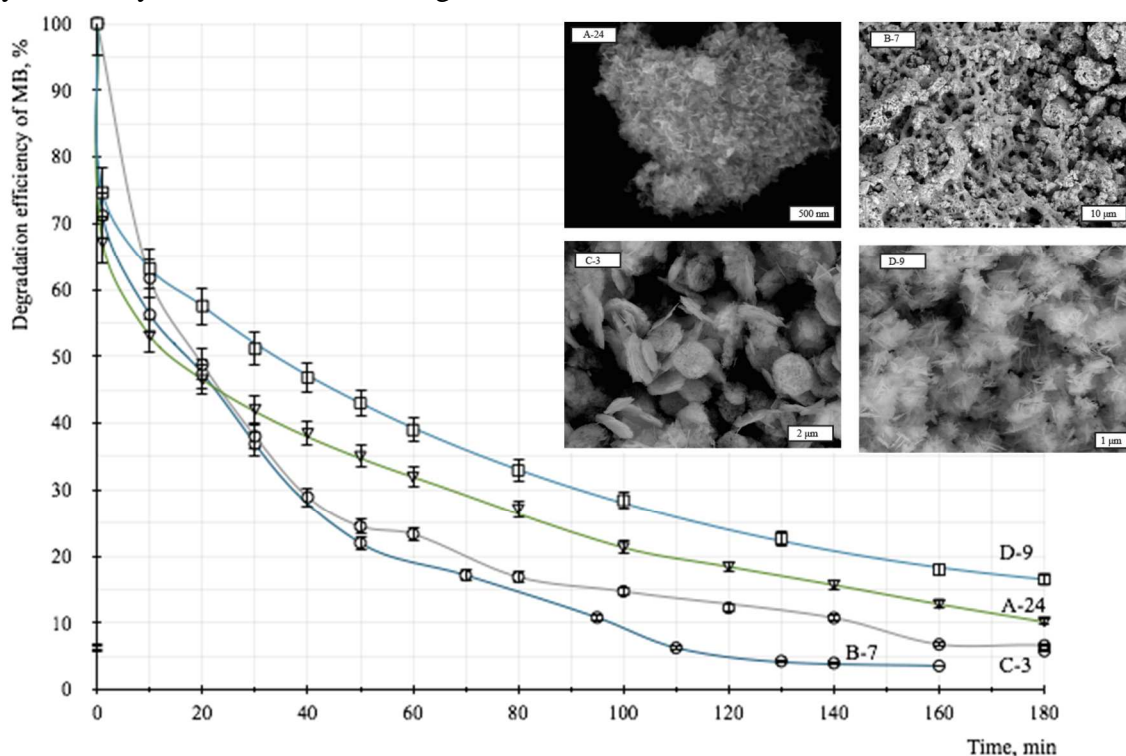


Fig. 20. The photo degradation curves of methylene blue dye using various Bi<sub>2</sub>WO<sub>6</sub> samples with different morphology

The sample (D-9) that has been obtained in microwave synthesis has flake-like structure, which consists of smaller layered structures. Such sample shows for about 20% lower photocatalytic degradation efficiency comparing to the sample B-7. Sample B-7 degrades approximately 90% of methylene blue after 100 minutes. It can be concluded that microwave synthesis produces high purity tungstate in a short time, however from the particle morphology view such type catalysts shows reduced photocatalytic activity. Samples B-7 and C-3 are obtained at higher temperature and reaches 90% and 85% degradation of methylene blue after 100 minutes respectively. Samples, which are thermally treated, have shown higher photocatalytic activity, and the reason for that is the increase of the sample crystallinity.

In case of zinc tungstate, the impact of the particle morphology on the methylene blue degradation is more expressed (Figure 21). Particles, which are obtained at higher pressure in microwave and hydrothermal conditions, are smaller and aggregated but with a higher specific surface area comparing to samples obtained from sol-gel combustion synthesis (sample B-25) and molten salt synthesis (sample A-4). The degradation curves show that photocatalytic activity of ZnWO<sub>4</sub> changes depending of particle morphology.

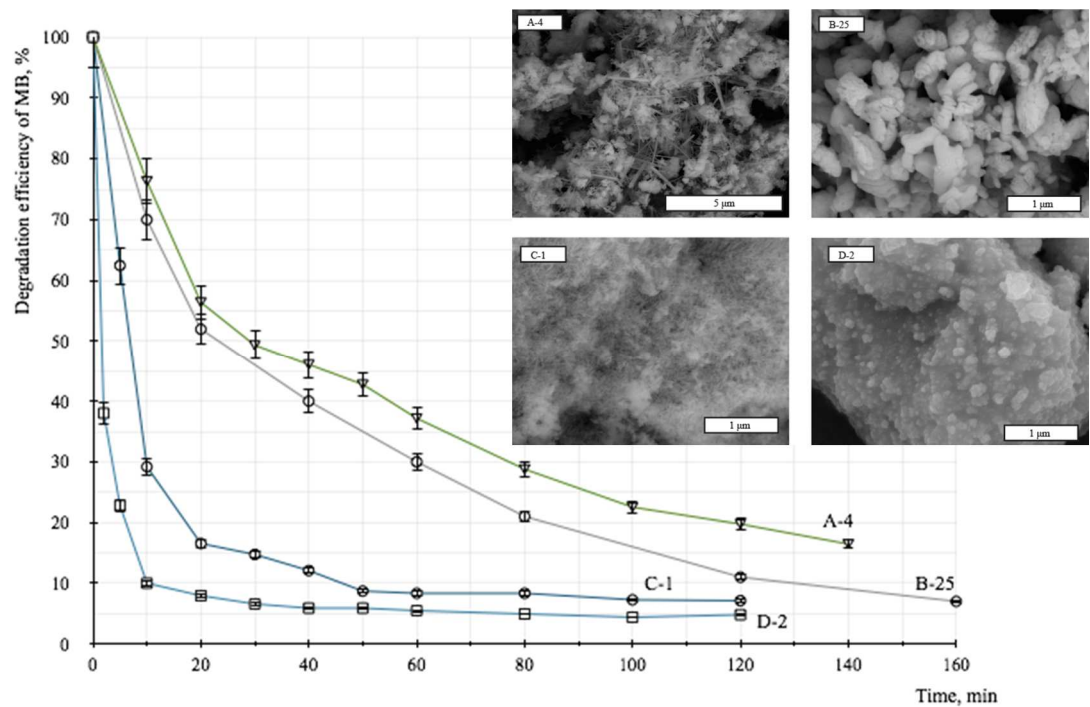


Fig. 21. The photo degradation curves of methylene blue dye using various  $ZnWO_4$  samples with different morphology

The different synthesis techniques and parameters led to structures with variable photocatalytic activity, which is confirmed by degradation curves of methylene blue. It can be concluded that degradation process of methylene blue is significantly affected by the morphology of the photocatalysts. By linking this to the synthesis techniques, it has been confirmed that bismuth tungstate with layered/elongated crystals shows lower photocatalytic activity than agglomerated structures obtained at 500 °C temperature. While zinc tungstate obtained with hydrothermal and microwave synthesis are more efficient for 20-25% comparing to the obtained product from sol-gel or molten salt synthesis.

## 10. The influence of the specific surface area and crystallite size on the degradation of methylene blue

It can be concluded that degradation rate constant depending on the specific surface area for pure zinc and bismuth tungstate are affected (Figure 22). For higher specific surface area the rate of methylene blue degradation are more efficient which is confirmed by increase of the degradation rate constant. For  $Bi_2WO_6$  photocatalysts it can be seen that photocatalytic degradation rate increases at specific surface area of 17-18  $m^2/g$ . Similarly, for the  $ZnWO_4$  photocatalytic activity shows at specific surface area higher than 28  $m^2/g$ . This means that for effective photocatalysis it is recommended to use  $Bi_2WO_6$  nanoparticles with specific surface area higher or equivalent with 18  $m^2/g$ , but  $ZnWO_4$  nanoparticles with specific surface area higher or equivalent with 28  $m^2/g$ .

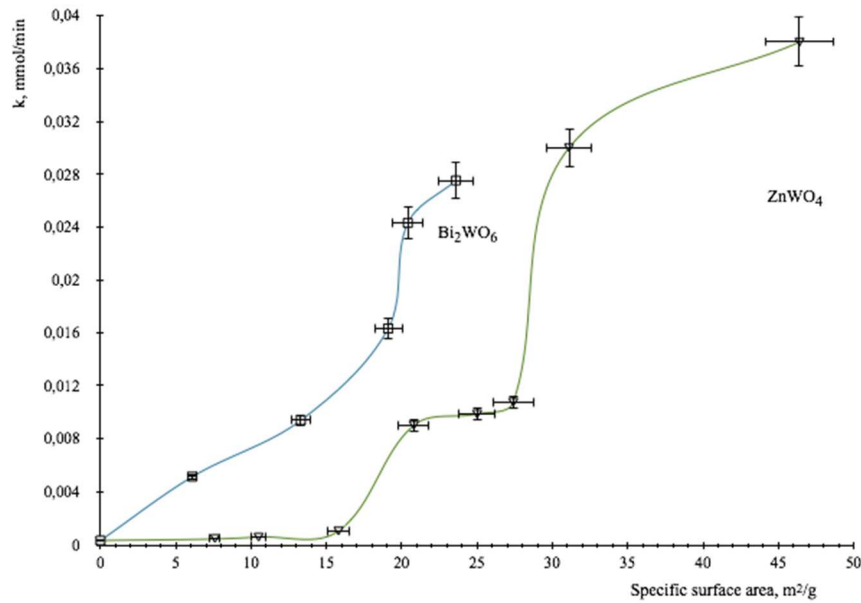


Fig. 22. The influence of the specific surface area on the degradation of methylene blue with different photocatalysts

There are significant differences between both types of photocatalysts. It can be seen that bismuth tungstate behaves more active than zinc tungstate. Such disparity is explained by the differences of the band gaps.

### 11. The influence of the pH on the degradation of MB

The results show that bismuth tungstate has the most efficient MB degradation at pH 7 (Fig. 23), which is around to its zero point of charge (pH ~6.7). The influence of the pH on photocatalytic processes is explained with strong impact of H<sup>+</sup> and OH<sup>-</sup> groups. Experiments showed that bismuth tungstate at pH<7 can disproportionate. While pH>7 affect the MB adsorption on the catalyst surface, which decreases the photocatalytic efficiency. Similar processes and results are obtained for zinc tungstate.

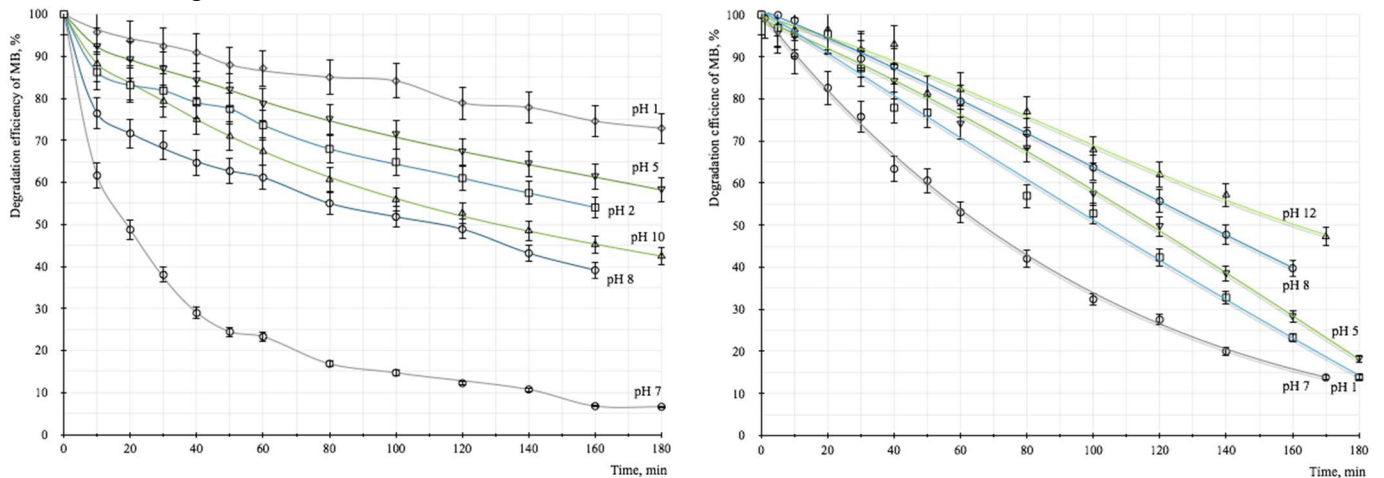


Fig. 23. The degradation curves of MB at different pH using  $\text{Bi}_2\text{WO}_6$  as photocatalyst (sample B-10 with SSA  $23.4 \text{ m}^2/\text{g}$ )

Fig. 24. The degradation curves of MB at different pH using  $\text{ZnWO}_4$  as photocatalyst (sample B-13 with SSA  $19.1 \text{ m}^2/\text{g}$ )

The change of pH affects also MB degradation in case of  $\text{ZnWO}_4$  photocatalyst (Fig. 24). It has been shown that more efficient MB degradation occurs at neutral pH by degrading of 75% of MB during 2 h of photocatalysis experiment (sample B-13, SSA= $19.1 \text{ m}^2/\text{g}$ ). The basic and acidic environment decreases the degradation efficiency, which is affected by  $\text{H}^+$  and  $\text{OH}^-$  ions.

Experiments show that using the luminescent daylight source, relatively high photo induced MB degradation occurs. The photocatalytic process is slower than using UV irradiation but this can be explained because of the lower photon energy. The difference is approximately 25% between UV irradiated and daylight source, after 2 h photocatalytic processing time (Figure 25).

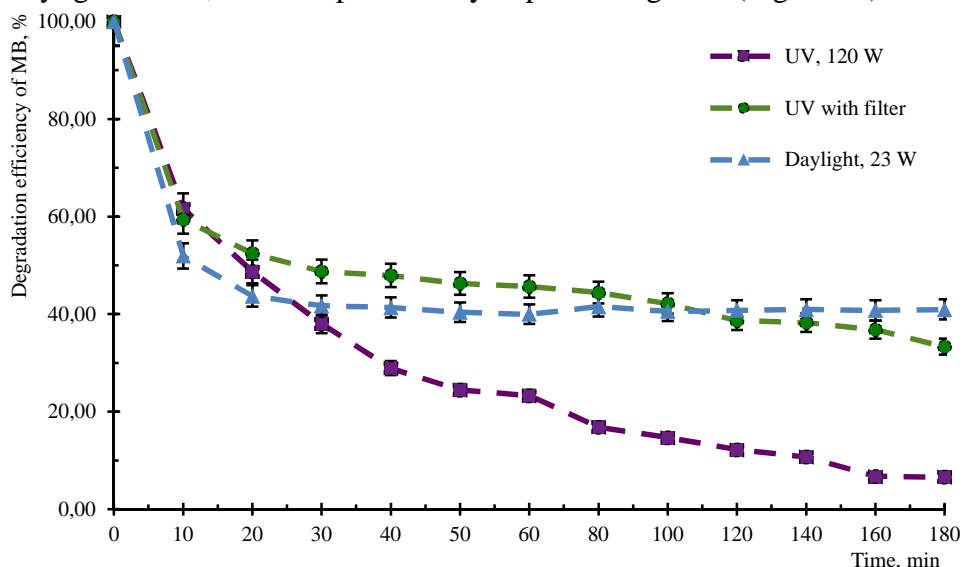


Fig. 25. Degradation curves of photocatalytic MB degradation using  $\text{Bi}_2\text{WO}_6$  as photocatalyst (sample B-10, SSA= $23.4 \text{ m}^2/\text{g}$ ) and different light sources

## 12. Photocatalysis of reprocessed and regenerated samples

The optimal frequency of reprocessed photocatalysts has been studied. By intervals of 130 minutes the repeatedly used catalyst ensures up to 70% of MB degradation also after four photocatalysis experiments. However, longer experiment time is necessary to reach higher efficiency (Fig. 26). For example, bismuth tungstate with specific surface area  $23.4 \text{ m}^2/\text{g}$  (sample B-10) at 70-minute time point of the 3<sup>rd</sup> cycle shows degradation of MB up to 50%, while the efficiency of the same time point at 1<sup>st</sup> cycle is almost two times higher and reaches 90%. This means that effective usage of photocatalysts are in 1<sup>st</sup> and 2<sup>nd</sup> cycle but in the 3<sup>rd</sup> and 4<sup>th</sup> cycles reduces for approximately 20%. The decrease of activity is explained by the MB adsorption on the catalyst surface.

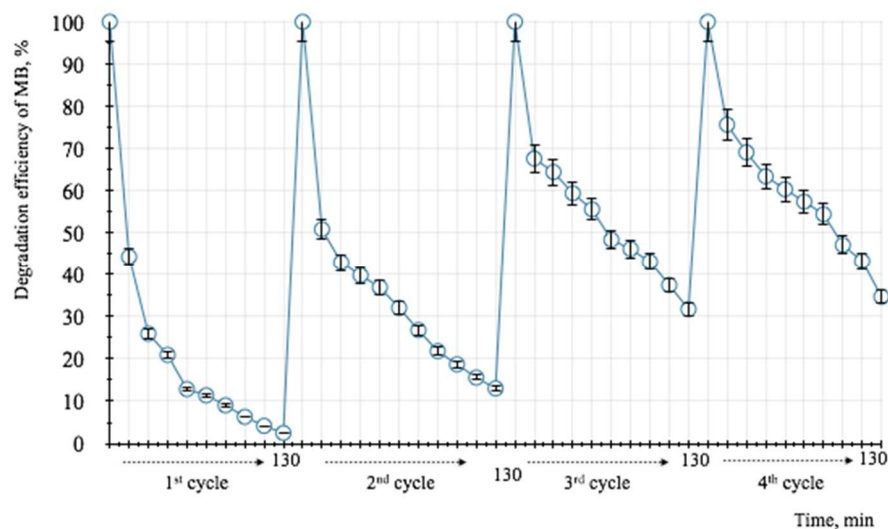


Fig. 26. Degradation curves of MB degradation using regenerated  $\text{Bi}_2\text{WO}_6$  as photocatalyst (sample B-10,  $\text{SSA}=23.4 \text{ m}^2/\text{g}$ )

### 13. Evaluation of the MB degradation products

During photocatalysis the decolouration of the MB solution can be observed which is improved by UV-VIS spectra and the intensity of MB spectral lines 664 nm and 292 nm decreases. For MB degradation product analysis the chromatographic analysis was performed before and after 90-minutes photocatalysis. Chromatograms analysis showed the intensive signal at retention time 6.7 min corresponding to the methylene blue, which is also confirmed by the UV-VIS spectra of methylene blue. While peak with retention time 3.4 min is leucomethylene blue (the reduced form of MB).

After 90-minutes photocatalysis, new signals in chromatograms are detected with various retention times (2.2 min, 3.4 min, 5.2 min, 5.9 min, 6.3 min, 6.7 min and 9.0 min, Fig. 27) and the intensity of the methylene blue peak has decreased while MB solution is decolorized.

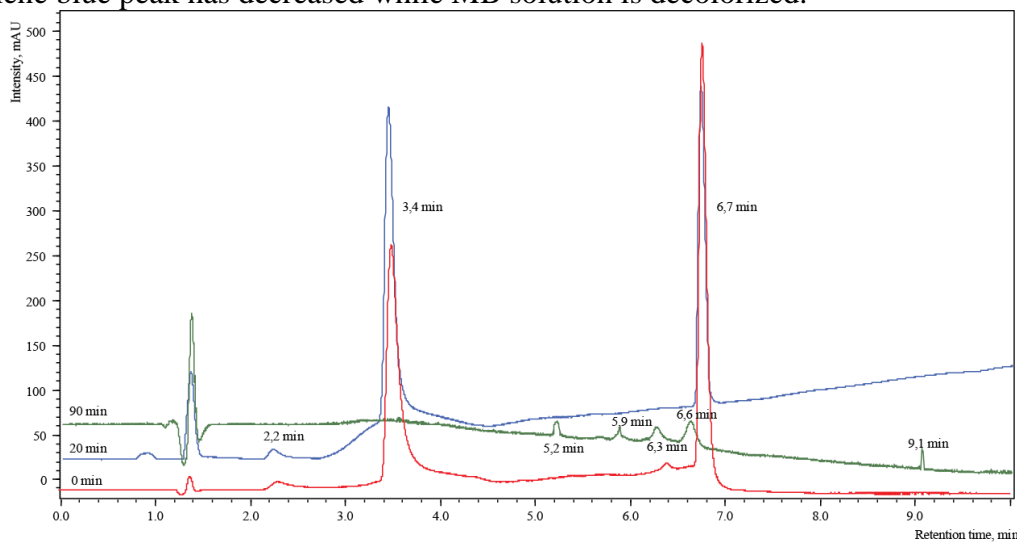


Fig. 27. MB sample chromatograms depending on photocatalysis time (wavelength 400-700 nm)

High performance liquid chromatography has proved that during MB photocatalysis new molecules are detected. Due to the complicated sample solution matrix the chromatograms are with

high background noise. Sample solution consists of compounds and ions with different characteristics and amounts creating interactions that cause undesirable conditions and side effects during HPLC analysis. Also the inorganic anions significantly interfere and cause the baseline shift of the chromatogram. The HPLC analysis gives superficial information about MB photocatalysis process. However, using carbon fibre micro extraction together with gas chromatography and mass selective (GC/MS) detector the MB degradation products was successfully analysed. Several intermediates of MB degradation were identified using GC/MS method.

GC/MS method is suitable for partial identification of the photocatalytic intermediates and the quantitative analysis is more complicated due to the complex matrix of the sample solution, which also contains inorganic anions. Based on the literature data, potential final degradation products are  $\text{SO}_4^{2-}$ ,  $\text{NH}_4^+$ ,  $\text{NO}_3^-$  ions,  $\text{CO}_2$  and water, which amount increase in the final steps of photocatalysis and is the main reason for complicated chromatography analysis (identification and quantification). Despite of that, it is demonstrated that photocatalysis finalizes by creating the  $\text{SO}_4^{2-}$ ,  $\text{CO}_3^{2-}$ ,  $\text{NO}_3^-$  ions using qualitative ion reactions (Table 6).

Table 6

The qualitative inorganic ion determination after MB photocatalytic degradation

Nr.	Ion	0 min	90 min	Possible origin
1	$\text{CO}_3^{2-}$	-	+	From $\text{CO}_2$ which dissolved in water
2	$\text{SO}_4^{2-}$	-	+	From sulphur in MB molecule in the presence of photocatalysis
3	$\text{NO}_3^-$	-	+	From nitrogen in MB molecule in the presence of photocatalysis
4	$\text{NH}_4^+$	-	-	From nitrogen in MB molecule in the presence of photocatalysis

It is concluded that used tungstate photocatalysts degrades organic compounds in the presence of photo irradiation, which is confirmed by the analysis of the degradation products. Huge role is for selected photocatalyst and initiated energy, as well as irradiation time for the successful and complete photodegradation of organic compounds.

## CONCLUSIONS

1. The NaCl-KCl, NaNO<sub>3</sub>, K<sub>2</sub>SO<sub>4</sub>-Na<sub>2</sub>SO<sub>4</sub> and NaCl-KCl, KCl, KNO<sub>2</sub> molten salts with lower melting temperature should be used for the effective single phase ZnWO<sub>4</sub> and Bi<sub>2</sub>WO<sub>6</sub> compounds and providing smaller crystallite size, respectively. The lowest pure bismuth tungstate synthesis temperature is 350°C using potassium nitrite, but the lowest temperature for obtaining pure zinc tungstate in molten salts is 350°C using sodium nitrate.
2. For obtaining single-phase bismuth tungstate, the glycerine and glycine, as organic fuel should be used, but for obtaining zinc tungstate all studied organic fuels (glycine, ethylene glycol, citric acid, ethanol) can be used. For obtaining smaller crystallites and higher specific surface area it is suggested to use the ratio org/NO<sub>3</sub><sup>-</sup> near to 0,67.
3. Microwave and hydrothermal synthesis provide obtaining of the pure tungstate at 180°C temperature, 5-10 bar pressure, in 20-240 minutes.
4. The optimal method for obtaining ZnWO<sub>4</sub> and Bi<sub>2</sub>WO<sub>6</sub> with high specific surface area (for ZnWO<sub>4</sub> up to 46,4 m<sup>2</sup>/g, for Bi<sub>2</sub>WO<sub>6</sub> up to 29,8 m<sup>2</sup>/g) and smaller crystallite size is in acidic or neutral synthesis environment using microwave synthesis at 180°C temperature.
5. The different synthesis techniques and parameters lead to structures with variable photocatalytic activity; the degradation process of methylene blue is significantly affected by the morphology of the photocatalysts. The plate-like/elongated crystals shows lower photocatalytic activity than agglomerated structures for bismuth tungstate.
6. The photocatalytic activity and degradation of MB depends on specific surface area of the powders and Bi<sub>2</sub>WO<sub>6</sub> nanoparticles with specific surface area >18 m<sup>2</sup>/g, but ZnWO<sub>4</sub> nanoparticles with specific surface area >28 m<sup>2</sup>/g should be used for effective photocatalysis.
7. The most effective degradation of MB is in neutral environment at pH 7 but optimum frequency of using the same photocatalyst can be reached in 1<sup>st</sup> – 2<sup>nd</sup> cycle.
8. From used dopants, the most effective degradation of MB is for photocatalysts that are doped with silver oxide, molybdenum and yttrium up to 1 wt%.
9. The obtained tungstate photocatalysts in the presence of light degrades organic compounds and potential degradation products of MB are SO<sub>4</sub><sup>2-</sup>, NH<sub>4</sub><sup>+</sup>, NO<sub>3</sub><sup>-</sup> ions, CO<sub>2</sub> and water.

## THESIS FOR DEFENDING

1. The crystalline zinc and bismuth tungstate nanoparticles with specific surface area of 46.4 m<sup>2</sup>/g and 29.8 m<sup>2</sup>/g, respectively and crystallite sizes of 17 nm, has be obtained from salt solutions by microwave synthesis at 180°C temperature, with pressure 13 bar in 20 minutes.
2. The effective zinc tungstate nanoparticle photocatalyst with specific surface area of higher than 28 m<sup>2</sup>/g and uniform particle distribution has been obtained using developed microwave and hydrothermal synthesis.
3. The effective bismuth tungstate nanoparticle photocatalyst with specific surface area of higher than 18 m<sup>2</sup>/g and with flowerlike particle morphology has been obtained using developed microwave and hydrothermal synthesis.

## LIST OF PUBLICATIONS

1. Kodols M., Didrihsone S., Grabis J., Bi<sub>2</sub>WO<sub>6</sub> Nanoparticles Prepared by Combustion Synthesis with Different Fuels and their Photocatalytic Activity, *Key Engineering Materials*, 2014, Vol. 604, 93-101, (SCOPUS)
2. Kodols M., Didrihsone S., Grabis J., The Influence of Different Molten Salt Systems on Zinc and Bismuth Tungstate Formation, *Key Engineering Materials*, 2014, Vol. 604, 142-145, (SCOPUS)
3. Grabis J., Jankovica D., Kodols M., Rašmane D., Photocatalytic activity of ZnWO<sub>4</sub> nanoparticles prepared by combustion synthesis, *J. of Latvian Chemistry*, 2012, Vol. 51 (1-2), 93-98
4. Kodols M., Didrihsone S., Grabis J., Comparison of Nanosized Bi<sub>2</sub>WO<sub>6</sub> Photocatalysts Prepared By Different Methods, *Proceedings of scientific Conference of Young Scientists on Energy Issues*. Kaunas, Lithuania, May 29-31, 2013, 1-9
5. T. Šalkus, L. Šatas, A. Kežionis, M. Kodols, J. Grabis, V. Vikhrenko, V. Gunes, M. Barre, Preparation and investigation of Bi<sub>2</sub>WO<sub>6</sub>, Bi<sub>2</sub>MoO<sub>6</sub> and ZnWO<sub>4</sub> ceramics, *Solid State Ionics*, 2015, Vol. 271, 73-74 (SCOPUS)
6. Serga V., Kulikova L., Cvetkov A., Chikvaidze G., Kodols M., Extractive-Pyrolytic Method for Au/MeO<sub>x</sub> Nanocomposites Production, *Key Engineering Materials*, 2014, Vol. 604, 118-121, (SCOPUS)
7. Dubnika A., Loca D., Reinis A., Kodols M., Berzina-Cimdina L., Impact of sintering temperature on the phase composition and antibacterial properties of silver-doped hydroxyapatite, *Pure and Applied Chemistry*, 2013 Vol. 85 (2), 453-462, (SCOPUS)
8. Serga V., Kulikova L., Cvetkov A., Krumina A., Kodols M., Chornaja S., Dubencovs K., Spruge E., Production of mono- and bimetallic nanoparticles of noble metals by pyrolysis of organic extracts on silicon dioxide, *IOP Conference Series: Materials Science and Engineering*, 2013, Vol. 49 (1), art. No. 012015, (SCOPUS)
9. Kronkalns G., Kodols M., Maiorov M. M., Structure, composition and magnetic properties of ferrofluid nanoparticles after separation, *Latvian Journal of Physics and Technical Sciences*, 2013, Vol. 50 (4), 56-61 (SCOPUS)
10. Zalite I., Heidemane G., Kodols M., Grabis J., Maiorov M., The synthesis, characterization and sintering of nickel and cobalt ferrite nanopowders, *Medziagotyra*, 2012, Vol. 18 (1), 3-7, (SCOPUS)

## LIST OF SCIENTIFIC CONFERENCES

1. Kodols M., Didrihsone S., Grabis J., Rozenberga L., The Influence of Different Molten Salt Systems on Zinc and Bismuth Tungstate Formation, *22<sup>nd</sup> International Baltic Conference of Engineering Materials and Tribology*, Riga, Latvia, November 14-15, 2013, 4
2. Didrihsone S., Kodols M., Grabis J., The influence of temperature and pH of Bi<sub>2</sub>WO<sub>6</sub> photocatalyst nanopowder formation, of abstracts of *28<sup>th</sup> Scientific Conference of Institute of Solid State Physics*, University of Latvia, February 8 – 10, 2012, Riga, Latvia
3. Grabis J., Jankoviča D., Kodols M., Rašmane D., Photocatalytic Activity of ZnWO<sub>4</sub> Nanoparticles Prepared by Combustion Synthesis, *Abstract book of XIX-th International Baltic Conference, Materials Engineering & Balttrib 2010*”, 28-29 October, 2010, Riga, Latvia, 14
4. Kodols M., Didrihsone S., Grabis J., Synthesis of Bi<sub>2</sub>WO<sub>6</sub> Photocatalyst Nanopowders with Modified Sol-Gel Method, *Abstract book of Training School Synthesis of Hybrid Organic-Inorganic Nanoparticles for Innovative Nanostructured Composites*, Naples, Italy, 28 February - 2 March 2011
5. Kodols M., Didrihsone S., Grabis J., Bi<sub>2</sub>WO<sub>6</sub> Photocatalyst Nanopowder Synthesis and Photodegradation of MB, *Abstract book Conference for Young Scientists "The Ninth Students"*

- Meeting, SM-2011" and "The Second ESR Workshop, COST MP0904", November 16-18, 2011, Novi Sad, Serbia, 49*
6. Kodols M., Didrihsone S., Grabis J., Synthesis of Bi<sub>2</sub>WO<sub>6</sub> Photocatalyst Nanopowders with Wet Chemical Methods, *20<sup>th</sup> International Baltic Conference "Materials Engineering 2011": Book of Abstracts*, October 27-28, Kaunas, Lietuva, 2011, 46
  7. Kodols M., Didrihsone S., Grabis J., Synthesis of Bi<sub>2</sub>WO<sub>6</sub> Photocatalyst Nanopowders with Wet Chemical Methods, *International Conference "Functional Materials and Nanotechnologies" (FM&NT-2011): Book of Abstracts*, April 5-8, 2011, Riga, Latvia, 229
  8. Serga V., Kulikova L., Cvetkov A., Krūmiņa A., Kodols M., Čornaja S., Dubencovs K., Sproģe E., Production of Mono- and Bimetallic Nanoparticles of Noble Metals by Pyrolysis of Organic Extracts on Silicon Dioxide. International Conference "Functional Materials and Nanotechnologies" (FM&NT-2013): Book of Abstracts, University of Tartu, Estonia, April 21-24, 2013, 110
  9. Serga V., Kulikova L., Cvetkov A., Chikvaidze G., Kodols M., Extractive-Pyrolytic Method for Au/MeO<sub>x</sub> Nanocomposites Production, *22<sup>nd</sup> International Baltic Conference of Engineering Materials and Tribology*, November 14-15, 2013, Riga, Latvia, 15
  10. Merijs Meri R., Zicans J., Biteniekis J., Zalite I., Heidemane G., Kodols M., Knite M., On the structure and relaxation properties of polycarbonate/ferrite nanocomposites - Book of Abstracts, *32. International conference „Composite materials in industry (SLAVPOLIKOM) and seminar „Pipelines from polymer composite materials: manufacturing, design, installation and exploitation”* June 6-11, 2012, Jalta, Ukraina, 412
  11. Merijs Meri R., Zicans J., Biteniekis J., Zalite I., Heidemane G., Kodols M., M. Knite. On the structure and relaxation properties of polycarbonate/ferrite nanocomposites, *32. Int. Conf. „Composite materials in industry (SLAVPOLIKOM) and seminar „Pipelines from polymer composite materials: manufacturing, design, installation and exploitation”* June 6-11, Yalta, Ukraine, 2012, 1
  12. Merijs Meri R., Zicans J., Biteniekis J., Zalite I., Heidemane G., Kodols M., Knite M.. Structure and properties of chemically synthesized ferrites and magnetic composites based on polycarbonate. *XI International Conference of Nanostructured Materials (NANO 2012), August 26-30, Rodos, Greece, 2012*
  13. Kronkals G., Kodols M., Maiorov M. M., Change of phase composition of magnetic fluid nanoparticles after HGMS, *Proceedings of 8th PAMIR International Conference on Fundamental and Applied MHD*, September 5 - 9, 2011, Borgo, France 955 – 959
  14. Maiorov M., Kronkalns G., Kodols M., Lubane M., Blums E., Fractionation and size determination of ferrite nanoparticles, International Conference "Functional Materials and Nanotechnologies" (FM&NT-2011): Book of Abstracts, April 5-8, 2011, Riga, Latvia, 184
  15. Zalite I., Kodols M., Heidemane G., Grabis J., Zicans J., Merijs-Meri R., Maiorov M.M., Bledzki A.K., The nickel and cobalt ferrite nanopowders and its composites with polycarbonate, *Multiphase Polymers and Polymer composites: From Nanoscale to macro Composites*, June 7 - 10, 2011, Paris, France
  16. Kodols M., Zalite I., Heidemane G., Grabis J., Maiorov M., Zicans J., Merijs-Meri R., The Synthesis and Characterization of Nickel and Cobalt ferrite Nanopowders and its composites with polycarbonates, *Abstract book of COST Action MP0701 Workshop, Nanoparticles Surface (Modified/Unmodified) as a base for the interaction with polymer matrix*, September 23 – 24, 2010, Novi Sad, Srbija

17. Kodols M., Zālīte I., Heidemane G., Grabis J., Maiorov M., The synthesis and characterization of nickel and cobalt ferrite nanopowders, *Abstract book of 11<sup>th</sup> International Conference on Ceramic Processing Science*, August 29-September 1, 2010 Zurich, Switzerland
18. Zālīte I., Grabis J., Kodols M., Zicāns J., Merijs-Meri R., Polycarbonate composites with Nickel and Cobalt ferrite Nanopowders, *Abstract book of XIX-th International Baltic Conference, Materials Engineering & Balttrib 2010*, October 28.-29, 2010, Riga, Latvia, 51

Patents:

19. Zālīte I., Grabis J., Palčevskis Ē., Kodols M., Zicāns J., Merijs-Meri R., Biteniēks J., Bočkovs I., Paņēmiens ferītu nanodaļiņu ieguvei polimēru nanokompozītu izgatavošanai, LV patents Nr. LV 14264, Int. Cl B82Y30/00